Fish and Shellfish Immunology 93 (2019) 597–611

Contents lists available at ScienceDirect

Fish and Shellfish Immunology

journal homepage: www.elsevier.com/locate/fsi

Full length article

# Insight into the molecular function and transcriptional regulation of activator protein 1 (AP-1) components c-Jun/c-Fos ortholog in red lip mullet (*Liza haematocheila)*

N.D. Janson[a,b], Nilojan Jehanathan[a], Sumi Jung[a,b], Thanthrige Thiunuwan Priyathilaka[a], Bo-Hye Nam[c], Myoung-Jin Kim[a,b,**], Jehee Lee[a,b,*]

[a] Department of Marine Life Sciences & Fish Vaccine Research Center, Jeju National University, Jeju Self-Governing Province, 63243, Republic of Korea
[b] Marine Science Institute, Jeju National University, Jeju Self-Governing Province, 63333, Republic of Korea
[c] Biotechnology Research Division, National Institute of Fisheries Science, 408-1 Sirang-ri, Gijang-up, Gijang-gun, Busan, 46083, Republic of Korea

ARTICLE INFO

*Keywords:*
JNK
AP-1
c-Jun
c-Fos
UV-Response
Immunity

ABSTRACT

The transcription factor, activator protein-1 (AP-1), is a dimeric protein and a downstream member of the mitogen-activated protein kinase (MAPK) signaling pathway. It regulates a wide array of functions including, cell proliferation, survival, differentiation, response to UV-irradiation, immune responses, and inflammatory conditions. AP-1 belongs to the basic leucine zipper (bZIP) protein family, which consists of members from Jun, Fos, Maf, and ATF subfamilies. In the present study, *c-Jun* and *c-Fos* homologs were identified from a transcriptome database of *Liza haematocheila* and designated as *Lhc-Jun* and *Lhc-Fos*. In both sequences, the signature bZIP domain was identified and also the DNA binding sites, dimerization sites, as well as the phosphorylation sites, were found to be highly conserved through evolution. Tissue distribution analysis revealed that both *Lhc-Jun* and *Lhc-Fos* transcripts were ubiquitously expressed in all examined tissues of healthy mullets. In order to determine the transcriptional modulations of *Lhc-Jun* and *Lhc-Fos,* challenge experiments were carried out using LPS, poly I:C, and *L. garvieae*. The qRT-PCR analysis revealed significant upregulation of *Lhc-Jun* and *Lhc-Fos* in blood, gill, liver, and spleen. This is the first study that explores the correlation between UV-irradiation and AP-1 ortholog expression in teleosts. Also, this is the first time that the functional characterization of the teleost c-Fos ortholog has been carried out. Sub-cellular localization of Lhc-Jun and Lhc-Fos was observed in the nucleus. AP-1-Luc reporter assays revealed significant higher luciferase activities in both Lhc-Jun and Lhc-Fos proteins compared to mock controls. These results strongly suggest that *Lhc-Jun* and *Lhc-Fos* might play a significant role in *Liza haematocheila* immunity by regulating AP-1 promoter sequences in immune and stress-related genes.

## 1. Introduction

Activator protein-1 (AP-1) was the first identified mammalian transcription factor that plays a significant role in cellular proliferation, differentiation, apoptosis, survival, and immune response [1,2]. It is a dimeric protein that comprises members of Fos (Fos-B, c-Fos, Fra-1, and Fra-2), Jun (Jun-B, c-Jun, and Jun-D), Maf (musculoaponeurotic fibrosarcoma), and ATF (activating transcription factor) protein families [3]. AP-1 forms different combinations of homo and heterodimers using Jun, Fos, Maf, and ATF proteins [4]. Moreover, AP-1 is a leucine zipper (bZIP) protein, which contains a highly conserved basic DNA binding region and leucine zipper for dimerization [5]. This specific dimerization and structural complexity together, with transcriptional and post-translational modification imparts AP-1 with the ability to regulate a wide array of cellular processes [3,4]. The mitogen-activated protein kinase (MAPK) pathway is responsible for the induction of AP-1 by phosphorylation [6]. Also, the cascade of MAPK activates AP-1 through a wide array of stimuli, such as growth factors, cytokines, neurotransmitters, viral and bacterial infections, apoptotic signals, and different environmental stresses such as UV irradiation and oxidative stress [7–9].

In the Jun family, c-Jun is the most puissant transcriptional

* Corresponding author. Marine Molecular Genetics Lab, Department of Marine Life Sciences, Jeju National University, Jeju Self-Governing Province, 63243, Republic of Korea.
** Corresponding author. Marine Molecular Genetics Lab, Department of Marine Life Sciences, Jeju National University, Jeju Self-Governing Province, 63243, Republic of Korea.
*E-mail addresses:* mj.kim@jejunu.ac.kr (M.-J. Kim), jehee@jejunu.ac.kr (J. Lee).

https://doi.org/10.1016/j.fsi.2019.08.013
Received 23 January 2019; Received in revised form 29 July 2019; Accepted 6 August 2019
Available online 07 August 2019
1050-4648/ 

activator while the c-Jun N-terminal kinase (JNK), a subgroup of MAPKs regulates c-Jun expression [10]. The c-Fos is a mainstream member of the Fos protein family which forms a stable dimer with c-Jun to form the AP-1 transcription factor [5,11,12]. While Fos proteins are unable to homodimerize, the Jun/Fos heterodimer complexes have a high affinity in binding to the AP-1 site of the target gene compared to the weak Jun/Jun homodimers [13]. Furthermore, c-Fos and c-Jun are the cellular homologs of retroviral oncogenes, which are involved in the oncogenic transformation of cells [1].

The innate immune system plays a vital role in many organisms as the first line of host defense [14]. The transcription factors, including AP-1, NF-κB (Nuclear factor- κB) and, IRF (Interferon Regulatory Factor) are mainly involved in the innate immune response against infectious pathogens [15]. AP-1 is primarily involved in the regulation of cytokine expression and inflammation via different cell signaling pathways such as TNF (tumor necrosis factor), RIG (retinoic acid-inducible gene-I-like receptors) and TLRs (Toll-like receptors) in response to different stimuli like pro-inflammatory cytokines and genotoxic stress [3,16]. AP-1 binds to the DNA sequence motifs, either TPA (phorbol 12-O-tetradecanoate-13-acetate) [5′TGAG/CTCA-3’] or cAMP (cyclic adenosine monophosphate) responsive elements [5′TGACGTCA-3’], and thereby regulates cytokine expression and inflammation by selectively expressing a wide range of genes in different cell types [3,17–19].

Till now, the only characterization study of AP-1 homolog in fish has been c-Jun characterization from Orange-spotted grouper (*Epinephelus coioides*) [20]. However, several c-Jun/c-Fos homologs have been studied in Molluscs [21–23], Arthropods [24–27], and Mammals [1,28]. The upregulation of the c-Jun homolog of Orange-spotted grouper has been observed under the Singapore grouper iridovirus (SGIV) challenge, where the researchers had performed subcellular localization and luciferase reporter assays to understand the functional traits of the c-Jun homolog [20]. Mollusc Jun homolog (AbJun) has been identified from *Haliotis discus discus;* this study has shown a significant upregulation of AbAP-1 in gill tissues upon a bacterial or viral hemorrhagic septicemia virus (VHSV) challenge [21]. Also, the studies on c-Jun/c-Fos homologs of *Litopenaeus vannamei* show the involvement of viral replication and viral gene expression in response to white spot syndrome virus (WSSV) infection [24]. Furthermore, some studies have suggested that the orthologs of c-Jun/c-Fos are involved in activation of the antimicrobial peptide (AMPs) expression in *Drosophila* [29], *Litopenaeus vannamei* (Pacific white shrimp) [25] and juvenile fine flounder (*Paralichthys adpersus*) [30]. On the other hand, previous work also suggests that AP-1 enhances the viral gene transcription or virus replication, such as activation of the viral immediate-early gene transcription of Human cytomegalovirus (HCMV), and replication of Hepatitis C virus (HCV) in hepatocarcinogenesis [31,32]. Collectively, these studies have resulted in confusing evidence by which it is indicated that c-Jun/c-Fos orthologs could play a protective or non-protective role in bacterial and viral infections [25].

Red lip mullet (*Liza haematocheila*) also known as *Chelon haematocheilus,* is a commercially available common species of fish in Korean waters. These fishes are widely spread in the northwestern Pacific inshore waters in Japan, Korea, and the coast of China [33]. *Liza haematocheila* belongs to family Mugilidae, and its diet includes polluted sediments. Due to this, *L. haematocheila* is considered the primary test organism for assessing the effect of estrogenic contaminants in the aquatic environments in Southeast Asia [34,35].

Though AP-1 and its components have been characterized in several invertebrates and mammals, research is scarce in fish AP-1 characterization. In order to fill that knowledge gap, c-Jun and c-Fos (AP-1) homologs (designated as Lhc-Jun and Lhc-Fos) in *L. haematocheila* were identified. For a better understanding of Lhc-Jun and Lhc-Fos characteristics and immune function, their spatial expression in different tissues was determined, and regulation of both genes upon lipopolysaccharide (LPS), polyinosinic:polycytidylic acid (poly I:C), and *Lactococcus garvieae* stimulations were studied. Furthermore, Lhc-Jun and Lhc-Fos were overexpressed in mullet kidney (MK) cells to determine their subcellular localization and reaction to activation of AP-1 responsive reporters. This is also the first instance which examine the *Lhc-Jun* and *Lhc-Fos* expression in fish cells upon exposure to UV light.

## 2. Materials and methods

### 2.1. Experimental subjects

#### 2.1.1. Experimental fish

Red lip mullet (*Liza haematocheila)* were purchased from Sangdeok fishery in Hadong Korea. The fish acclimatization process was done at 20 °C for one week in laboratory aquarium tanks before experimentation. All the experiments using the experimental animals were performed under the approval of Jeju National University animal experiment ethics committee (Approval no- 2018-003).

#### 2.1.2. Experimental cell

A mullet (*Liza haematocheila*) kidney cell line was created for the first time and used for subcellular localization, UV irradiation studies and AP-1-Luc assay. Mullet kidney was used for the primary cell culture. Briefly, kidney tissues were harvested from a healthy Red lip mullet with an average weight and length of 80 g and 21 cm, respectively. Harvested tissues were washed three times with 1X PBS and transferred to a sterile dish containing L-15 medium (Sigma) which was supplemented with 40% FBS (Hyclone), 100 U/mL penicillin and 100 μg/mL streptomycin (1X P/S) (Gibco). The kidney tissues were minced and then filtered using a 40 μm cell strainer (SPL). Single cells, separated from kidney tissue, were then seeded in a 6-well plate and incubated at 25 °C. On a daily basis, the cell condition was checked, and half of the medium was replaced. After three days, the medium was changed to L-15 medium, supplemented with 20% FBS and 1X P/S and after 7 days, it was replaced with normal complete medium (L-15 with 10% FBS and 1X P/S). Subculture was started when the cell populations exhibited stable growth. All experiments were performed within 20 passages.

### 2.2. Construction of cDNA database and identification of Lhc-Jun and Lhc-Fos

The *de novo* assembly technique was used to construct the mullet cDNA transcriptome database. Concisely, tissue sample from blood, spleen, kidney, head kidney, gill, skin, stomach, intestine, brain, heart, eye, and liver were collected from five mullets as mentioned in section 2.4 and total RNA was extracted from each tissue (section 2.6). The extracted RNA was sent for sequencing, where sequencing was done on a Pacbio platform at Insilicogen, Korea. *Lhc-Jun* and *Lhc-Fos* sequences were identified from the constructed transcriptome database using the Basic Local Alignment Search Tool (BLAST) (http://blast.ncbi.nlm.nih.gov/Blast.cgi), National Center for Biotechnology Information (NCBI), [36].

### 2.3. Bioinformatics analysis

The open reading frame (ORF) and the amino acid (aa) sequences of putative Lhc-Jun and Lhc-Fos were predicted using the NCBI (ORF) finder (https://www.ncbi.nlm.nih.gov/orffinder/) [37]. The ExPASy prosite (http://prosite.expasy.org/) [38], NCBI-CDD (https://www.ncbi.nlm.nih.gov/Structure/cdd/wrpsb.cgi) [39], and Motif Scan (http://myhits.isb-sib.ch/cgi-bin/motif_scan) online servers were used to predict the Lhc-Jun and Lhc-Fos domain architectures. The physiochemical properties such as molecular weights and isoelectric points of Lhc-Jun and Lhc-Fos were estimated by the ExPASy ProtParam tool [40]. The PSORT II (https://psort.hgc.jp/form2.html) sever was used to predict the Nuclear Localization Signal (NLS) [41]. The identified Lhc-

Jun and Lhc-Fos ortholog sequences were found by BLAST searches. Ortholog sequences were compared by ClustalW [42] in the BioEdit software and Multiple Sequence Alignment (MSA) was constructed. Pairwise alignments were performed using the EMBOSS needle pairwise sequence alignment tool (https://www.ebi.ac.uk/Tools/psa/emboss_needle/) [43]. Neighbor-joining method of MEGA 7.0 [44] was used for the phylogenetic analysis of Lhc-Jun, Lhc-Fos and their orthologs, using 5000 bootstrapped replicate trails. The 3-D structure of the monomeric form of the two proteins was predicted using the RaptorX web portal (http://raptorx.uchicago.edu/StructurePrediction/predict/) [45]. The tertiary structure of the functionally important domain (bZIP) and the dimerization between Lhc-Jun and Lhc-Fos were predicted by SWISS-MODEL online platform using the homology-based modeling technique [46]. The partial X-ray crystallographic structure of human transcription factor Fos/Jun domain complex (PDB: 5vpf.1) was used as the template to build the model. PyMOL molecular visualization system was used to fine-tune the models that were built [47].

### 2.4. Tissue sampling

Acclimatized animals were used for tissue sampling. Five healthy mullet fish, with average weight and length of 100 g and 24 cm, respectively were used. Fish were anesthetized using MS-222; 40 mg/L. Whole blood was collected using heparin-coated (USB, USA) sterile syringes. Subsequently, the samples were immediately centrifuged at 3,000 × g for 10 min at 4 °C, to separate peripheral blood cells from plasma, and directly snap-frozen. The liver, head kidney, gill, spleen, brain, intestine, kidney, muscle, stomach heart, and skin were excised and immediately snap-frozen in liquid nitrogen. The samples were stored at −80 °C until total RNA extraction.

### 2.5. Pathogen challenge experiment

Acclimatized healthy mullets were separated into four groups of fish where each group contained 25 fish. Three groups were separately injected intraperitoneally by 1.5 μg/g of polyinosinic:polycytidylic acid (poly I:C) (Sigma-Aldrich, USA), 1.25 μg/g of lipopolysaccharide (LPS) (Sigma-Aldrich, USA), and $1 \times 10^3$ CFU/μL of *Lactococcus garvieae*. These stimulants were prepared in sterile phosphate-buffered saline (PBS), and 100 μL of each solution was injected into the respective animals. The remaining control group was injected with PBS. Tissue samples from the liver, gill, spleen, and peripheral blood cells were collected from each group (n = 5) at time points of 0, 6, 24, 48, 72 h post-injection and stored as described previously (section 2.4).

### 2.6. Total RNA extraction and cDNA synthesis

The collected tissue samples from the healthy fish group (n = 5), and challenged fish groups along with the control group (n = 5), for each time point, were measured and pooled separately. The pooled tissue samples were used to extract total RNA using RNAiso plus (TaKaRa, Japan) followed by a RNeasy spin column (Qiagen, Germany) purification. The RNA quantification was done using a μDrop Plate (Thermo Scientific) by measuring the absorbance at 260 nm. Moreover, the quality of the RNA was confirmed by performing gel electrophoresis in a 1.5% agarose gel. PrimeScript™ II 1st strand cDNA Synthesis Kit (TaKaRa, Japan) was used to synthesize the first strand cDNA. The cDNA was synthesized using 2.5 μg of RNA along with the kit in a 20 μL reaction mixture. The synthesized cDNA samples were diluted 40 fold using nuclease-free water and stored at −80 °C for future analysis.

### 2.7. Transcriptional analysis of Lhc-Jun and Lhc-Fos by using quantitative real-time PCR (qRT-PCR)

Expressions of *Lhc-Jun* and *Lhc-Fos* in normal and immune challenged fish were analyzed by qRT-PCR using the synthesized cDNA (section 2.6). The Dice™ TP800 Real Time Thermal cycler System (TaKaRa) was used for the qRT-PCR, in a total volume of 10 μL of reaction mixture containing 3 μL of diluted cDNA template, 5 μL of 2X SYBR® Premix Ex Taq™ (TaKaRa, Japan), 0.4 μL of gene-specific primers (10 pmol/μL) (Suppl. Table 1, qPCR primers), and 1.2 μL of PCR-grade $dH_2O$. The qPCR cycle comprised of, 5 min of initial denaturation at 95 °C followed by 40 cycles of 95 °C for 5 s, 58 °C for 10 s, 72 °C for 20 s, and a dissociation cycle at 95 °C for 15 s, 60 °C for 30 s, and 95 °C for 15 s. Each qPCR reaction was performed in triplicates. The experiments were conducted following the Minimum Information for Publication of Quantitative Real-Time PCR Experiment (MIQE) guidelines [48]. The specificity of the PCR products was confirmed by analyzing the dissociation curve, and the mRNA expression level of *Lhc-Jun* and *Lhc-Fos* were determined using the Livak ($2^{-\Delta\Delta Ct}$) method [49]. The *Liza haematocheila* Elongation Factor 1 alpha (*LhEF1-α*) (MH017208) was subjected to the same qPCR conditions as the internal control, and gene expression levels were compared to obtain the relative gene expression values of *L. haematocheila*. In the immune-challenged group, relative changes in the *Lhc-Jun* and *Lhc-Fos* expression levels were determined by normalizing with the PBS injected control at corresponding time points. Further, the uninjected control (0 h) was considered as the baseline to calculate relative fold difference of *Lhc-Jun* and *Lhc-Fos* expression.

### 2.8. Construction of Lhc-Jun and Lhc-Fos recombinant plasmids

For the functional characterization of Lhc-Jun and Lhc-Fos proteins, both *Lhc-Jun* and *Lhc-Fos* were cloned into pcDNA™3.1(+) (Invitrogen™, USA) and pEGFP-N1(CLONTECH) cloning vectors. Specific primers with corresponding restriction sites were designed to amplify the *Lhc-Jun* and *Lhc-Fos* coding sequences (Suppl. Table 1, cloning primers). The synthesized cDNA (section 2.6) from muscle (for *Lhc-Jun*) and liver (for *Lhc-Fos*) tissues were used as the template for the PCR reaction. The PCR reaction mixture was prepared in a total volume of 50 μL containing 3 μL of cDNA template, 4 μL of dNTP mixture (2.5 mM), 5 μL of 10 × ExTaq buffer, 1 μL of each forward and reverse primers, 0.2 μL of TaKaRa Ex Taq™ DNA polymerase (5 units/μL) (TaKaRa, Japan) and PCR grade sterilized distilled water. The primer annealing temperatures were optimized using gradient PCR, and the optimized annealing temperatures were found to be 58 °C (Lhc-Fos primers) and 56 °C (Lhc-Jun primers). Using these annealing temperatures the following PCR thermal cycle was performed in a TaKaRa PCR thermal cycler Dice TP600 (TaKaRa, Japan): one cycle of 94 °C for 5 min (initial denaturation); 35 cycles of amplification at 94 °C for 30 s, 58 °C or 56 °C for 60 s, and 72 °C for 1 min, and a final extension at 72 °C for 7 min. Subsequently, the PCR products and the vectors [pEGFP-N1 and pcDNA™3.1(+)] were digested using corresponding restriction enzymes, and the digested product was purified using Accuprep™ purification kit (Bioneer Co., Korea). Next, ligation was performed at 16 °C for 30 min for both pEGFP-N1 and pcDNA™3.1(+) vectors using Mighty Mix (TaKaRa, Japan). The *Lhc-Fos* -GFP/pcDNA™3.1(+) and *Lhc-Jun* -GFP/pcDNA™3.1(+) recombinant constructs were transformed into *Escherichia coli* DH5α competent cells, and the positive colonies were sent for sequencing (Macrogen, Korea) The identity and the orientation of the sequences were confirmed by sequencing results. The QIAfilter™ plasmid Midi Kit (QIAGEN Germany) was used to prepare the sequence confirmed constructs for transfection.

### 2.9. Subcellular localization

Mullet kidney cells were cultured as mentioned in section 2.1. The cells were seeded in a 12 well plate ($2 \times 10^5$ cell/well). The MK cells were transfected with 1 μg of plasmid constructs *Lhc-Jun*-GFP, *Lhc-Fos*-GFP, and control pEGFP-N, using XtremeGENE™ 9 DNA transfection reagent (Roche, Germany) according to the manufacturer's instructions.

After 24 h incubation at 25 °C, the cells were washed with PBS thrice and fixed with 4% paraformaldehyde in room temperature for 10 min. Subsequently, the cells were stained for 5 min using 4,6-diamino-2-phenylindole (DAPI). The cells were observed under a fluorescence microscope (Leica, Germany).

### 2.10. Effect of UV irradiation on Lhc-Jun and Lhc-Fos expression

The UV irradiation effect on fish cell signaling was tested using the expression levels of *Lhc-Jun* and *Lhc-Fos*. The MK cells were cultured as mentioned in section 2.1.2 (90% confluency), followed by exposure to short wavelength UV radiation (254 nm) using HL-2000 HybriLinker (UVP®, UK). Both time and dose-dependent relative mRNA expressions were examined. The cells were exposed to an energy dosage of 40 J/$m^2$ (2 J/$m^2$/s for 20 s) and 80 J/$m^2$ (2 J/$m^2$/s for 40 s) and incubated in 25 °C together with a control group that was not exposed to UV. All cells from culture plates were harvested at two different time points (12 h, 24 h post-irradiation). The harvested cells were stored at −80 °C until RNA extraction. Following cell harvesting, total RNA was extracted from all experimental groups [*Lhc-Jun* and *Lhc-Fos* (12 h/40 J $m^{-2}$, 24 h/40 J $m^{-2}$, 12 h/80 J $m^{-2}$, 24 h/80 J $m^{-2}$)] using the RNeasy mini kit (QIAGEN, Germany), and cDNA was synthesized as mentioned in section 2.6. The *Lhc-Jun* and *Lhc-Fos* relative gene expression levels upon UV exposure were analyzed using qRT-PCR. The experiment was conducted using the synthesized cDNA from all five group of cells including the control group. The qRT-PCR was conducted as mentioned in the above section 2.8 using the same qRT-PCR primers for *Lhc-Jun*, *Lhc-Fos,* and *LhEF1-α* (Suppl. Table 1). The relative fold differences of *Lhc-Jun* and *Lhc-Fos* in each group was calculated compared to the untreated control. The experiments were performed in triplicates and data were presented as the mean standard deviation (SD).

### 2.11. Analysis of AP-1 activity using AP-1 Luc reporter gene

The activity of Lhc-Jun and Lhc-Fos at the AP-1 site was investigated using the AP-1 Luciferase reporter (AP-1-Luc) assay. Mullet kidney cells were cultured as mentioned in section 2.1.2 and cells were seeded in 6 well plates ($2 \times 10^5$ cells/well) and grown up to 90% confluency. For the transfection, 0.35 μg of expression plasmid constructs *Lhc-Jun*-pcDNA™3.1(+), *Lhc-Fos*-pcDNA™3.1(+) or empty pcDNA™3.1(+) vectors, with 0.2 μg of AP-1 reporter plasmid and 0.1 μg of Renila luciferase (pRL-TK) plasmid were used. Also in the co-transfection, 0.35 μg of both *Lhc-Jun*-pcDNA™3.1(+) and *Lhc-Fos*-pcDNA™3.1(+) were used. The total DNA amount for the transfection was maintained at 1 μg using pcDNA™3.1(+). Transfection was conducted using X-tremeGENE™ 9 DNA Transfection Reagent (Roche Diagnostics GmbH, Germany) following the manufacturer's guidelines. Transfected cells were incubated at 37 °C with 5% $CO_2$ for 48 h; cells were harvested using 1X Passive Luciferase Lysis Buffer 2.0 (Biotium, USA). The lysates were subjected to luciferase activity assay using Firefly & Renilla Luciferase Single Tube Assay Kit (Biotium, USA) according to the manufacturer's instructions. Luciferase activity was indicated as a relative fold value compared to the activity of the empty pcDNA™3.1(+) vector-transfected cells and Renila luciferase was used as the internal control.

### 2.12. Statistical analysis

The mean standard deviation ( ± SD) was used to represent all data, and all experiments were performed in triplicates. Two-tailed unpaired student's t-test or one-way analysis of variance (ANOVA) posthoc pairwise comparison test was used to distinguish the significance between groups having P value less than 0.05 ($P < 0.05$).

## 3. Results

### 3.1. Molecular properties, sequence and tertiary structure characterization of Lhc-Jun and Lhc-Fos

In the present study, *Lhc-Jun* and *Lhc-Fos* were identified from the transcriptome database of *Liza haematocheila* and characterized at the molecular level. The *Lhc-Jun* and *Lhc-Fos* sequence information are available in the GenBank database with accession numbers (MK225505, MK225506), respectively. The *Lhc-Jun* cDNA sequence was 2865 bp long with a 981 bp ORF encoding a polypeptide of 326 aa. Respectively, the theoretical molecular weight and the predicted Iso-electric point (pI) of Lhc-Jun polypeptide was 35.84 kDa and 8.65. The 1902 bp long cDNA of *Lhc-Fos* consists of an ORF of 1143 bp which encodes for 380 aa. The Lhc-Fos polypeptide was predicted to have a theoretical molecular weight of 41.2 kDa and a pI of 5.06. Meanwhile, Lhc-Jun contains two NLS (265–268: RKRK, 252–269: RKRMRNRIAASKCRKRK) and it is predicted to be 82.6% nuclear. The Lhc-Fos was also predicted to contain two NLS (114–130: KRGRGEQISPEEEEKRR, 132–148: RRERNKQAAAKCRNRRR) and was 73.9% nuclear. The domain architectures of Lhc-Jun and Lhc-Fos were studied to get a broad idea about the functional properties of these proteins. Lhc-Jun was found to possess a Transactivation domain (3–121 aa) comprising of residues Ser: 62,72 for phosphorylation (Phosphoacceptors: P) with critical site residues for both phosphoacceptors, Ser-62 (P + 1: Pro, P + 2: Asp, P + 4: Gly, P + 5: Cys), and Ser-72 (P + 1: Pro, P + 2: Glu, P + 4: Glu, P + 5: Arg) [50]. Whereas several phosphorylation sites of Lhc-Fos (Thr-232, 325, 331 and Ser-374) were identified at the carboxy-terminal and, the signature proline residue (+1P) was identified adjacent to serine or threonine at Thr-325, 331 and Ser-374 [51]. But, Lhc-Fos, Thr-232 residue was not followed by an adjacent proline. It was predicted that both Lhc-Jun and Lhc-Fos possesses the main bZIP domain (Lhc-Jun: 247–310 aa, Lhc-Fos: 126–189 aa). This bZIP domain consists of a basic region containing a DNA binding site, and a leucine zipper region comprising of a dimerization site (Fig. 1A and B). The predicted dimerized model of the bZIP domain in Lhc-Jun and Lhc-Fos (Fig. 1C) was similar to the crystal structure of the human heterodimeric bZIP transcription factor c-Fos, c-Jun identified by J. Glover and S. Harrison [52].

### 3.2. Sequence alignment and homology analysis

The homology between the different orthologs of c-Jun and c-Fos including Lhc-Jun, Lhc-Fos were analyzed using MSA (Fig. 2A and B, respectively). The critical amino acid residues were highly conserved throughout the vertebrate and invertebrate sequences. The putative NLS sequence sites (Lhc-Jun: 252–269 aa, Lhc-Fos: 114–130 aa, 132–148 aa) were well conserved among both vertebrates and invertebrates. The phosphorylation sites (phosphoacceptors- Ser 63/73) and nearby critical residues (P + 1, P + 2, P + 4, and P + 5) were highly conserved within c-Jun orthologs, and also the carboxy-terminal phosphorylation sites within the c-Fos orthologs were highly conserved among all the analyzed vertebrate orthologs (Thr-325, 331, and Ser-374). Ser-374 was found to be conserved in both vertebrates and invertebrates. The highest conservation was shown by the bZIP domains of all examined orthologs. The majority of the residues were similar among the other orthologs of c-Jun and c-Fos, and the pairwise alignment comparisons (Suppl. Table 2) further confirmed the resemblance between the sequences. Lhc-Jun showed the highest identity (93.6%) and similarity (96.3%) with that of *Epinephelus coioides*, while Lhc-Fos showed the highest identity (88.5%) and similarity (92.1%) with the *Seriola dumerili* protein.

### 3.3. The evolutionary relationship of c-Jun and c-Fos via phylogeny

Phylogenetic analysis of c-Jun and c-Fos orthologs were conducted

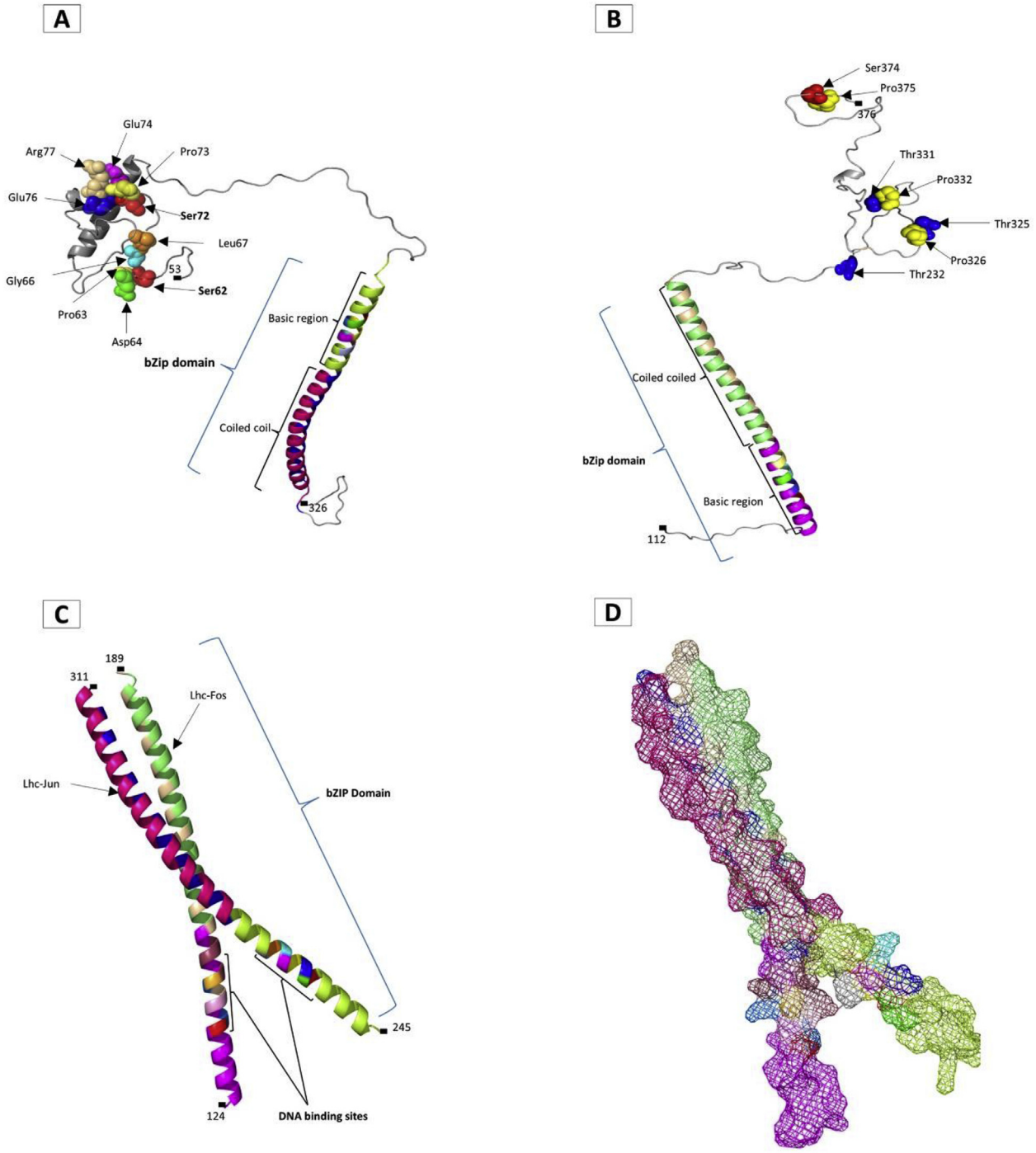


**Fig. 1.** The 3-D structure of the main catalytic region of (A) Lhc-Jun, (B) Lhc-Fos based on homology modeling technique. The phosphoacceptor and surrounding residues are shown as different colored spheres labeled in three-letter amino acid code. The Lhc-Jun and Lhc-Fos dimerized AP-1 b-ZIP domain is shown in (C) where the mesh structure of dimerized bZIP is shown in (D).

to study the relationship among the selected vertebrates and invertebrates through evolution. The phylogenetic trees constructed for both c-Jun and c-Fos contained two main clusters which conspicuously separate into vertebrates and invertebrates (Fig. 3A and B, respectively). Among the vertebrates, the fish orthologs were clustered into a separate clade while the amphibians, reptiles, birds, and mammals joined into a common clade in both c-Jun and c-Fos phylogenetic trees. The Lhc-Jun and Lhc-Fos orthologs joined the fish group and clustered with the highest phylogenetically related species studied, *Epinephelus coioides, Larimichthys crocea*, and *Seriola dumerili*, respectively.

### 3.4. Tissue-specific transcriptional pattern of Lhc-Jun and Lhc-Fos

The qRT-PCR results revealed that the mRNA expression levels of *Lhc-Jun* and *Lhc-Fos* were ubiquitous for all selected tissues under normal physiological conditions (Fig. 4). The highest expression of *Lhc-Jun* was in muscle, brain, and heart (12.31, 7.54, 7.13 fold) while stomach, spleen, kidney, and gill showed moderate expression levels (3.66, 3.15, 2.97, 2.26 fold). Moreover, head kidney and intestine demonstrated the least expression of *Lhc-Jun* (Fig. 4A). In the *Lhc-Fos* mRNA expression profile, the highest expression was detected in the liver (45.22 fold). The kidney, gill, heart, brain exhibited moderate

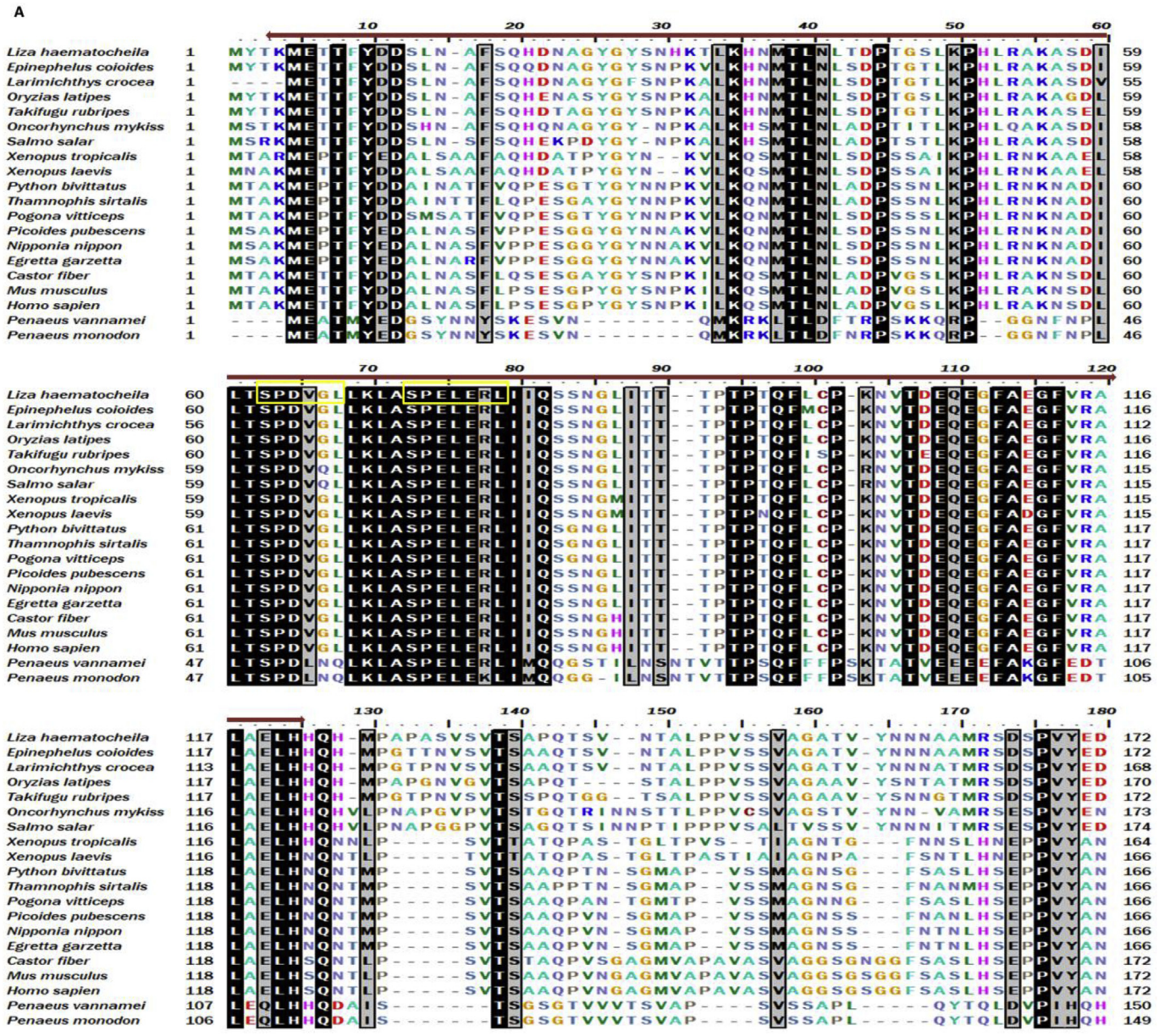


**Fig. 2.** Multiple sequence alignment of the deduced amino acid sequences of (A) Lhc-Jun and (B) Lhc-Fos. The identical and similar sequences are highlighted in black and grey, respectively. The dashes denote the gaps in the alignment. The brown and blue double-headed arrow denotes the transactivation domain and bZIP domains respectively. The red and orange boxes indicate the basic and coiled-coil regions while purple stars and light green arrows, respectively, mark the residues for DNA binding and dimerization. The green arrowheads denote the phosphoacceptor residues and the surrounding residues are indicated by a yellow box.

expression (18.47, 15.06, 13.39, 13.02 fold respectively) while skin, muscles, spleen, and blood showed lower expression levels. The least expression of *Lhc-Fos* was observed in the stomach (Fig. 4B).

### 3.5. The temporal transcriptional response of Lhc-Jun and Lhc-Fos upon immune challenge

The temporal expressions of *Lhc-Jun* and *Lhc-Fos* were analyzed in blood, gill, liver and spleen tissues at different post injection (p.i) time points (6, 12, 24, 48, and 72 h p.i) after the LPS, poly I:C, *L. garvieae* immune challenge (Fig. 5). Upon the LPS challenge, the temporal expression profile of *Lhc-Jun* in blood and spleen revealed that *Lhc-Jun* level was upregulated at 24 h p.i (1.85, 1.86 fold, respectively compared to 0 h expression) while blood gave a maximum peak at 72 h p.i (2.24 fold). The gill showed a 1.72 fold late phase upregulation at 72 h p.i. Early phase upregulation was observed in the liver at 6 h p.i (2.0 fold) and showed a higher peak at 24 h p.i (2.31 fold) (Fig. 5A). During the poly I:C challenge all the tested tissues showed an upregulation of *Lhc-Jun*. Except for blood the other three tissues, gill, liver, and spleen exhibited an early phase upregulation at 6 h p.i (4.4, 2.5, and 1.27 fold, respectively), while a late-phase expression of 1.38 fold was observed in blood at 72 h p.i (Fig. 5B). Upon *L. garvieae* challenge blood and gill showed significant late phase upregulations and the highest peak at 72 h p.i (4.01, 2.00 fold). Spleen had a mid-phase upregulation at 24 h p.i, while a 1.3 fold early phase upregulation was detected in the liver at 6 h p.i (Fig. 5C).

Meanwhile, the expression profile of *Lhc-Fos* exhibited a mid-phase upregulation in all the tissues tested with LPS. A fold value of 6.0, 1.73, 4.26 and 1.6 was observed in blood, gill, liver, and spleen, respectively at 24 h p.i. The gill showed highest expression at 72 h p.i (3.79 fold) (Fig. 5D). The poly I:C challenge elevated the expression of *Lhc-Fos* to a peak at 24 h p.i in all tested tissues; blood: 3.97 fold, gill: 3.95, liver:

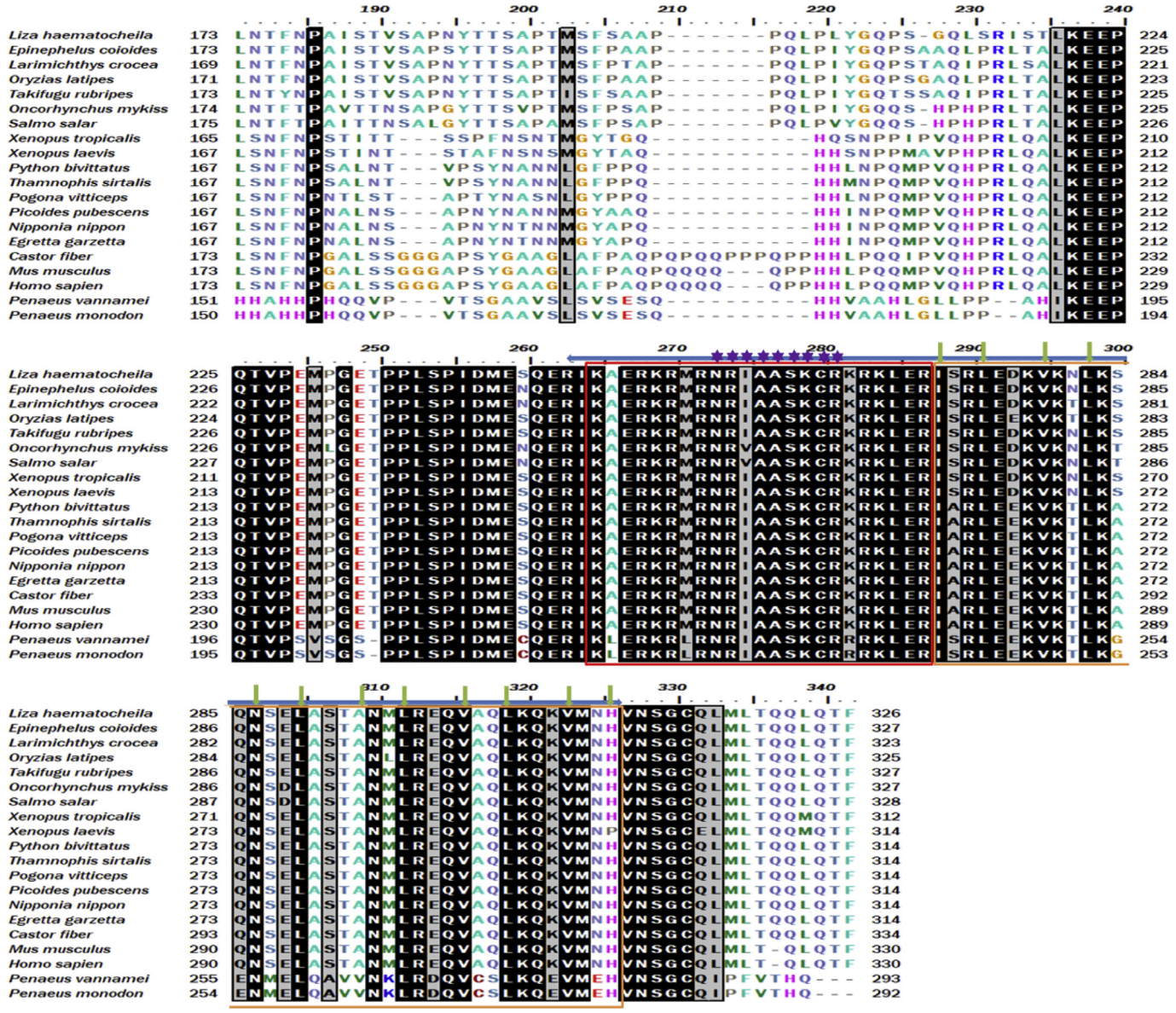


**Fig. 2.** (*continued*)

1.60 fold, and spleen: 4.10 fold compared to the control (Fig. 5E). After the *L. garvieae* injection, expression of *Lhc-Fos* showed a mid-late-phase peak in both blood and spleen at 48 h p.i (2.9 and 1.8 folds, respectively) while the liver showed a mid-phase stimulation at 24 h p.i (2.5 fold) and 1.7 fold upregulation in gill at 72 h p.i (Fig. 5F).

### 3.6. Subcellular localization assay

Fluorescence microscopy was used to examine the subcellular localization of Lhc-Jun and Lhc-Fos proteins. MK cells transfected with empty pEGFP-N-1 as the control showed a dispersed green fluorescence throughout the cell (Fig. 6A). The *Lhc-Jun*-GFP and *Lhc-Fos*-GFP transfected cells showed a green fluorescence exclusively in the nucleus (Fig. 6B and C), suggesting that Lhc-Jun-GFP and Lhc-Fos-GFP were localized to the nucleus.

### 3.7. Effect on Lhc-Jun and Lhc-Fos in response to UV irradiation

The effect of UV irradiation was examined by assessing the expression levels of *Lhc-Jun* and *Lhc-Fos* in UV irradiated MK cells. The qRT-PCR results showed both *Lhc-Jun* and *Lhc-Fos* were observed to be upregulated in both doses of UV light (40, 80 J $m^{-2}$) to a higher fold value compared to in control (Fig. 7). Also, the expression levels of both genes were observed to increase with time. *Lhc-Jun* expression in 40 J $m^{-2}$ low energy dose groups at 12 h and 24 h were 7.20 fold and 27.89 fold, respectively. Interestingly, the fold value of *Lhc-Jun* expression was reduced 24 h post radiation in 80 J $m^{-2}$ UV treated cells compared to the 12 h time point with the same energy dosage (12 h: 24.28 fold and 24 h: 10.60 fold) (Fig. 7A). *Lhc-Fos* showed an increment of fold value in a both dose and time-dependent manner. In 40 J $m^{-2}$ low dosage; 12 h: 3.71 fold, 24 h: 10.88 fold and in 80 J $m^{-2}$ high dosage 12 h: 8.30 fold, 24 h: 22.41 fold values were observed (Fig. 7B).

### 3.8. Effect of Lhc-Jun and Lhc-Fos on AP-1-Luc reporter activity

AP-1 reporter activity was analyzed using the luciferase assay. All three groups, *Lhc-Jun*, *Lhc-Fos,* and *Lhc-Jun* + *Lhc-Fos* co-transfected groups exhibited significantly higher activity fold values (3.29, 2.89, 4.25 folds, respectively) compared to the pcDNA control (Fig. 8).

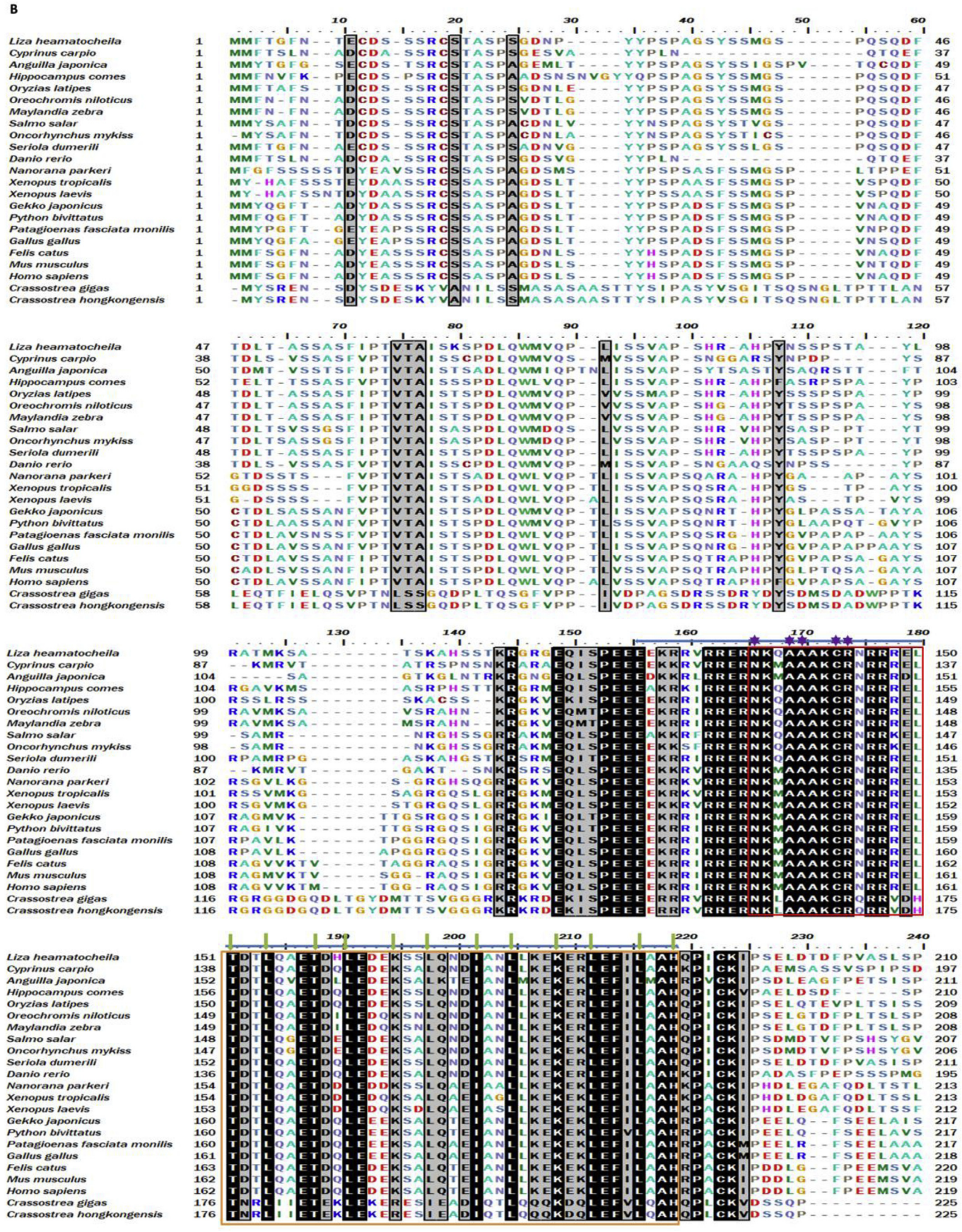


**Fig. 2.** (*continued*)

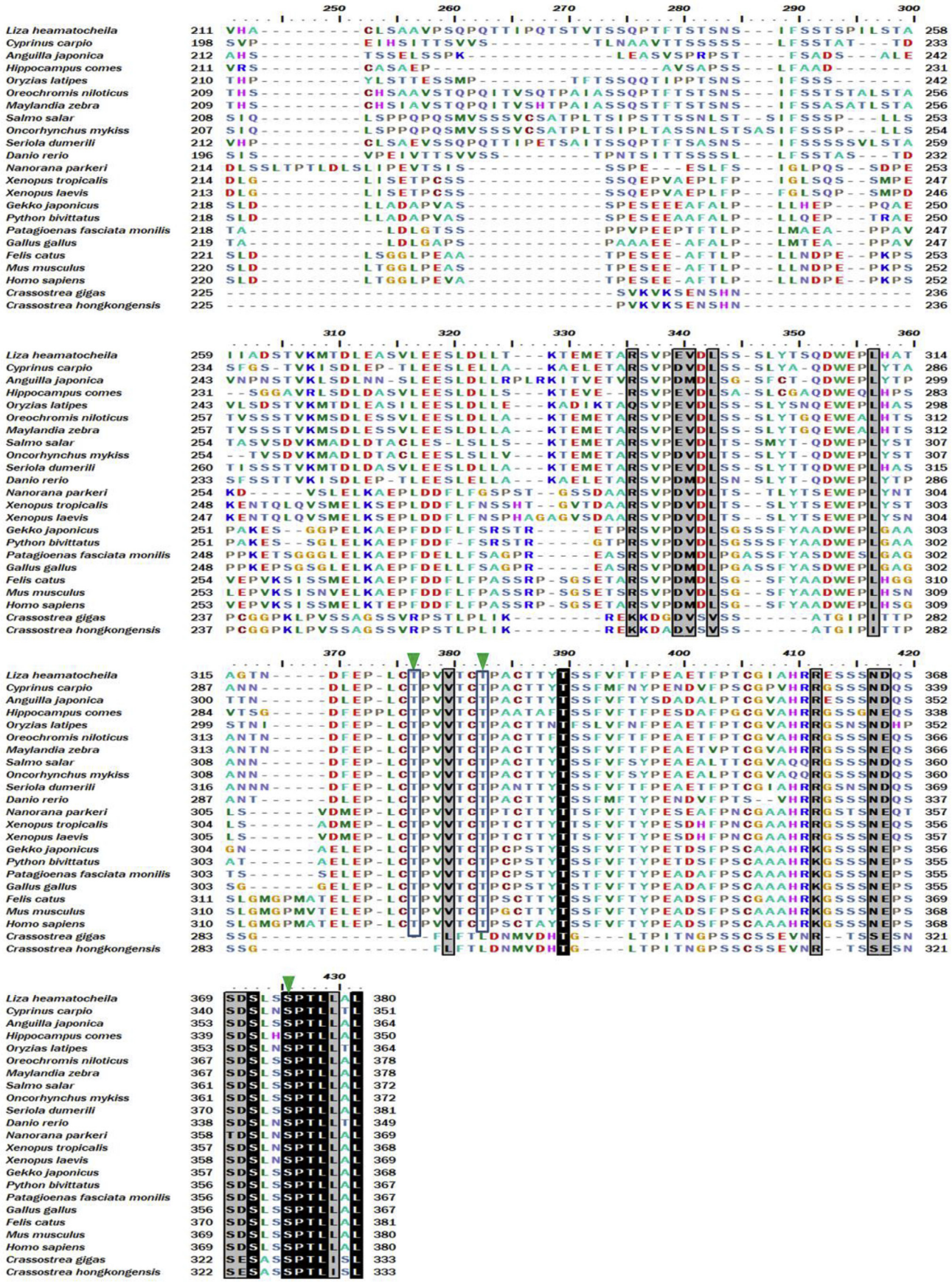


**Fig. 2.** (*continued*)

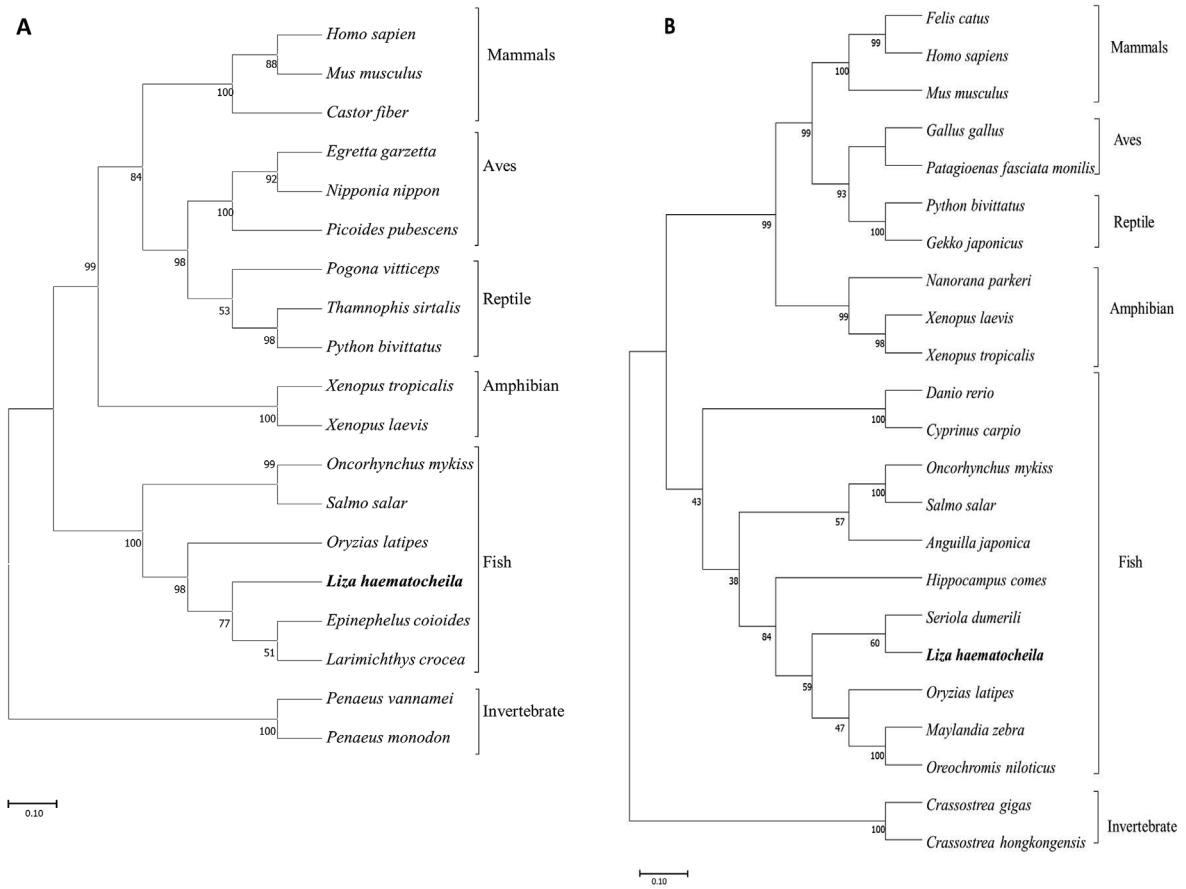


**Fig. 3.** Phylogenetic analysis of (A) Lhc-Jun, (B) Lhc-Fos with c-Jun and c-Fos orthologs of selected vertebrate and invertebrates. The analysis was performed by the neighbor-joining method using MEGA7.0 [44]; the bootstrap percentage is based on 5000 bootstrap replications, which are shown at the nodes of the tree. Accession numbers used in this study are given in Suppl. Table 2.

## 4. Discussion

AP-1 is one of the main transcription factors which is involved in a wide variety of cellular processes. AP-1 responds to a diverse array of signals, including growth factors, cellular stress, UV irradiation, neuronal depolarization, antigen-binding by T and B lymphocytes, and cytokines such as TNFα and interferon-γ [53]. The key components of AP-1 complex c-Jun and c-Fos have been associated with tissue injury, immune responses, and in stress response [10,53]. This significant immunological functionality led to this study, investigating the key components of the AP-1 ortholog (Lhc-Jun and Lhc-Fos) and their correlation to the host (*Liza haematocheila*) immune defense.

In this study, we have examined *Lhc-Jun* and *Lhc-Fos* in molecular, transcriptional, and functional levels. The Lhc-Jun and Lhc-Fos domain architecture plays a critical role in their functionality. The predicted Lhc-Jun and Lhc-Fos tertiary structures resembled the human c-Jun and c-Fos proteins [52], which results in the folding pattern conducive to their functionality. The presence of the primary domain (bZIP) in both Lhc-Jun and Lhc-Fos facilitated the dimerization and DNA binding by correctly positioning catalytic binding sites, as shown in Fig. 1, which mirrors the human orthologs [4,54]. It has been shown that this heterodimerization of c-Jun with c-Fos is 25 times more efficient in binding to its specific DNA than the homodimers formed with c-Jun itself [55]. The phosphorylation of the specific phosphoacceptors of Jun and Fos by JNKs or ERKs results in their activated forms [51,56]. Importantly, the human c-Jun phosphoacceptor sites Ser 63/73 and surrounding site residues closely resemble the Ser 62/72 and surrounding sequence of Lhc-Jun. Moreover, the carboxy-terminal MAPK phosphorylation sites and the surrounding residues of both human c-Fos and Lhc-Fos are similarly positioned [50,51]. These resembling positions and domain structure affirm the transcriptional activity of Lhc-Jun and Lhc-Fos. Also, this domain architecture indicates the manner in which the Jun and Fos dimers gained different DNA binding affinity, which regulates and links to various signal transduction pathways [55,57]. The MSA results further indicated that the critical functional domains and sites are highly conserved through the evolution, which confirmed the conservation of functional activities in Lhc-Jun and Lhc-Fos orthologs.

Phylogenetic analysis confirmed that the Lhc-Jun and Lhc-Fos sequences obtained were fish proteins. Among the selected vertebrate sequences; Lhc-Jun and Lhc-Fos were included in the fish group demonstrating its fish origin. This grouping could be attributed to the high identity and similarity values which Lhc-Jun and Lhc-Fos shared with other vertebrates and fish orthologs. An earlier study had shown a similar evolutionary pattern for c-Jun and c-Fos from orange-spotted grouper [20], rainbow trout [58] and silver carp [59]. These previous reports, along with our results, imply that both Lhc-Jun and Lhc-Fos proteins are homologous to other c-Jun, c-Fos orthologs, and both have originated from the fish group.

Spatial expression analysis of *Liza haematocheila* showed that *Lhc-Jun* and *Lhc-Fos* were ubiquitously expressed in all examined tissues. Gene characterization studies on *c-Jun* and *c-Fos* have shown a different level of expression pattern in fish and few invertebrates. The *Epinephelus coioides c-Jun* expression profile has demonstrated that *c-Jun* ortholog is expressed abundantly in gill, brain, and heart [20], whereas, in this study, *Lhc-Jun* was abundantly expressed in muscle, brain, and heart. Myogenic differentiation in mouse myoblast has shown significant *c-Jun* expression in mouse [60]. Also, a recent study showed *c-Jun*

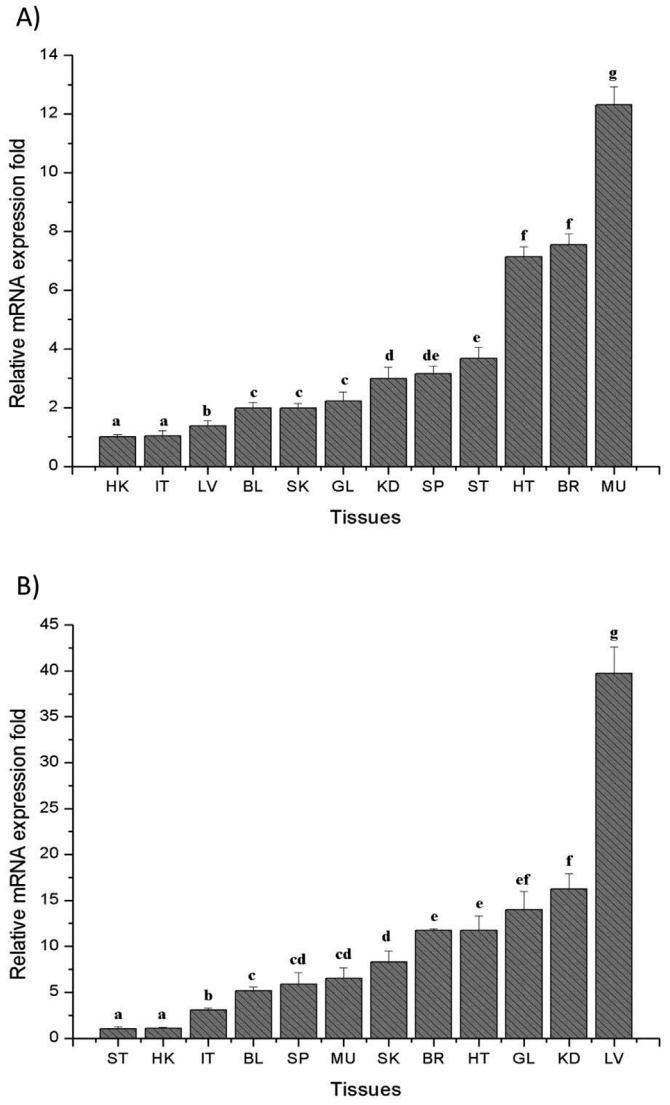


**Fig. 4.** The tissue distribution of (A) *Lhc-Jun*, (B) *Lhc-Fos* in head kidney (HK), intestine (IT), liver (LV), blood (BL), skin (SK), gill (GL), kidney (KD), spleen (SP), stomach (ST), heart (HT), brain (BR), and muscle (MU). The mRNA expression was measured by qRT-PCR and evaluated by the Livak method. *Liza haematocheila* EF1-α was used as the internal control. Error bars represent standard deviation with experimental replicates (n = 3). Significant differences are indicated by alphabets ($P < 0.05$).

expression in the skeletal muscle of juvenile fine flounder (*Paralichthys adpersus*) [30]. Furthermore, *c-Jun* expression in invertebrates *Litopenaeus vannamei* [24], *Penaeus monodon* [26], and *Crassostrea hongkongensis* [23] have been observed mainly in gill, hemocytes, hepatopancreas, mantle, and to a lesser extent in other tissues. The highest *Lhc-Fos* expression was observed in the liver. A similar expression profile has been reported in *c-Fos* ortholog of silver carp [59] where the liver shows the highest expression of *c-Fos*. Moreover, mouse hepatic gene studies have shown that following a hepatic injury or stress, c-Fos has to be expressed rapidly to maintain the liver metabolic homeostasis and limit tissue injuries [61]. All these findings suggest that tissue-specific expression of *c-Jun* and *c-Fos* is identical to all the species where abundant common expression can be observed in the liver, spleen, gill, blood, and brain.

In the case of pathogen infection, the innate immune system provides the first line of defense against an infectious agent [15]. Innate immunity of an organism is responsible for distinguishing the infectious foreign pathogens by its self-components using specific receptors like Toll-like receptors (TLRs). Subsequently, the signal is sent through the signal transduction pathways, and inflammatory response genes are activated using transcription factors like NF-κB, AP-1 [15]. This process initiates inflammatory responses in the host, which leads to the immobilization of the foreign pathogen and its destruction. During this process, transcription factor AP-1 plays a major role in activating a large number of genes as an immediate-early transcription factor [62]. In this study, the Lhc-Jun and Lhc-Fos involvement in the immune response of *Liza haematocheila* has been examined. The study was conducted after the fish was exposed to LPS, poly I:C and *L. garvieae* pathological stresses. LPS is a Gram-negative bacterial endotoxin [63]. Poly I:C was used to mimic a viral infection since it is a synthetic double-stranded viral RNA analog. *L. garvieae* was used as the live pathogen since it is a Gram-positive coccus causing severe economic loss to the mullet aquaculture industry [64,65]. After the challenge experiments, the mRNA expression profiles of *Lhc-Jun* and *Lhc-Fos* were examined in blood, gill, liver, and spleen tissues. These tissues have been recorded as some of the main immune tissues in fish [66,67]. The LPS challenge indicated that both *Lhc-Jun* and *Lhc-Fos* have an early mid-phase upregulation in all four tissues examined. LPS is identified by its physiological receptor TLR4-MD-2 complex, and it activates a cascade of intracellular signaling [63]. The identification of LPS by TLR4 rapidly activates NF-κB and all three MAPK pathways which are comprised of JNK, ERK, and p38 [68]. Then the signal subsequently passes on to the transcription factors (NF-κB, AP-1) to induce the pro-inflammatory cytokines [63,68]. Previous studies report that AP-1 (*c-Jun,* c-Fos) orthologs of *Crassostrea hongkongenesis* have shown a similar upregulation upon Gram-negative bacteria challenge in hemocytes [22,23]. Human primary macrophages have shown that AP-1 is involved in LPS induced expression of IL-6 and TNF [69]. This evidence suggests that *Lhc-Jun* and *Lhc-Fos* may be involved in immunity against Gram-negative bacterial pathogens. The early phase upregulation of *Lhc-Jun* in gill, liver, spleen, and the middle phase upregulation of *Lhc-Fos* in all tested tissues was significant in response to poly I:C challenge. Interestingly, this early-mid phase upregulation can be expected from *Lhc-Jun* and *Lhc-Fos* against poly I:C because of both act as an immediate-early transcription factor which is involved in innate immunity of fish [70]. Gene characterization studies of orange-spotted grouper [20] have shown a significant increment of a *c-Jun* ortholog in spleen upon Singapore grouper iridovirus (SGIV) infection. Since poly I:C is an analog of double-stranded viral RNA, it is recognized by TLR3 [71]. TLR3 signaling leads to the activation of pro-survival and pro-inflammatory transcription factors, AP-1 and NF-κB [72]. *Lhc-Jun* may also be involved in acquired immunity in the fish group. That would be the reason for the late phase upregulation peak in blood after poly I:C challenge. Previous studies have reported that the JNK pathway regulates T-cell activation and differentiation [73]. The role of AP-1 in leukocyte activation and differentiation in the immune system has been extensively studied (Foletta et al., 1998). It is a known fact that fish consist of T cells that are functionally similar to mammals, where T helper cells (Th cells) assist B cells and macrophages while Cytotoxic T cells (CTLs) kill virus-infected cells [74]. These evidence, along with our results suggest a strong role of *Lhc-Jun* and *Lhc-Fos* against viral infection in host defense. The green liver syndrome is a major defect caused by the *L. garvieae* in red lip mullets (*Liza haematocheila*) [64]. Results of this study demonstrated that upon *L. garvieae* challenge, liver *Lhc-Jun* and *Lhc-Fos* were upregulated in the early-mid phase. Together, both genes showed a late-mid phase upregulation in the blood and spleen, while both genes showed a late phase upregulation in the gill. The *L. garvieae* cause severe damage to the internal organs, including liver and spleen, which is one of the main mortality causing agents in mullet and rainbow trouts [75,76]. The intraperitoneal injection of *L. garvieae* leads to the rapid spreading of the bacteria in the peritoneum; this may be the reason for the early and mid-phase upregulation of *Lhc-Jun* and *Lhc-Fos* in blood, spleen, and liver. Studies have revealed the major role played by TLR2 in recognizing Gram-positive bacteria [77].

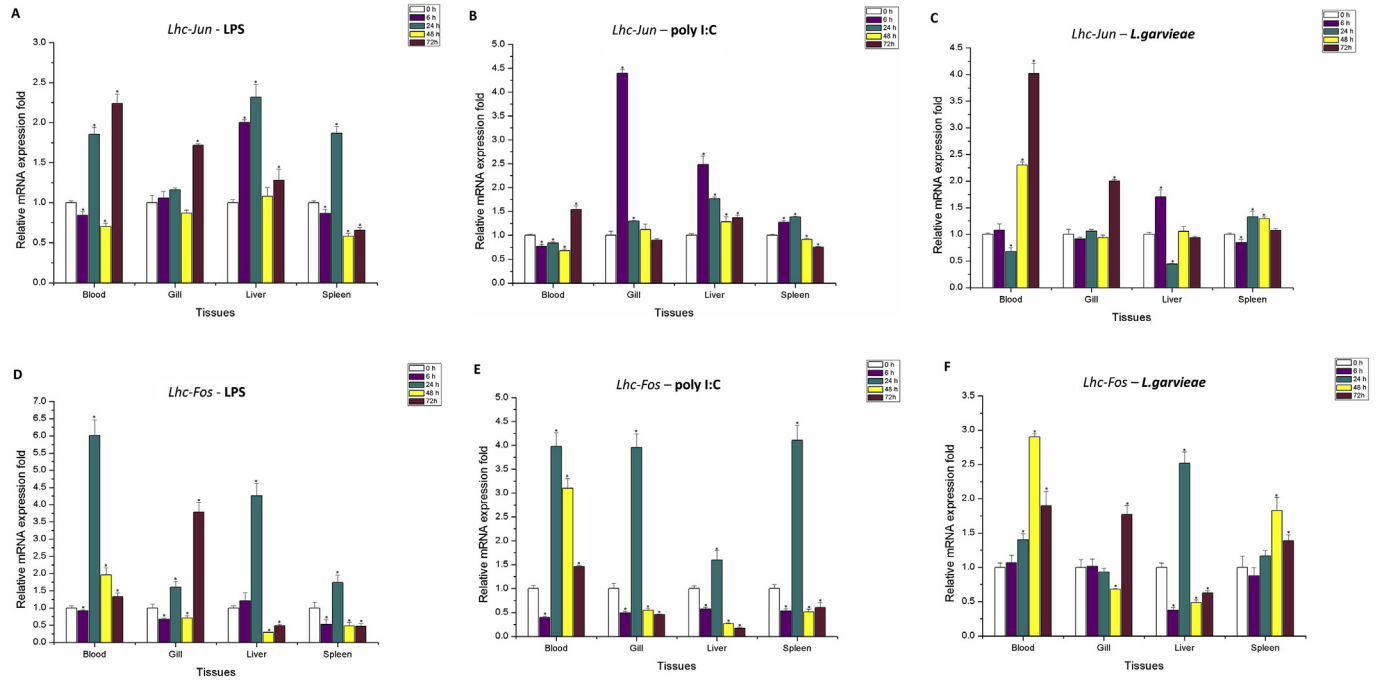


**Fig. 5.** The temporal expression profiles of *Lhc-Jun* and *Lhc-Fos* genes upon LPS, poly I:C, and *L. garvieae* in blood, gill, liver, and spleen during 0 h, 6 h, 24 h, 48 h, and 72 h post-challenge time points. The mRNA expression was measured by qRT-PCR and evaluated by the Livak method [49]. *Liza haematocheila* EF1-α was used as the internal control. Error bars represent standard deviation with experimental replicates (n = 3). Significant differences between challenged groups and 0 h control groups are indicated by an asterisk (*) ($P < 0.05$).

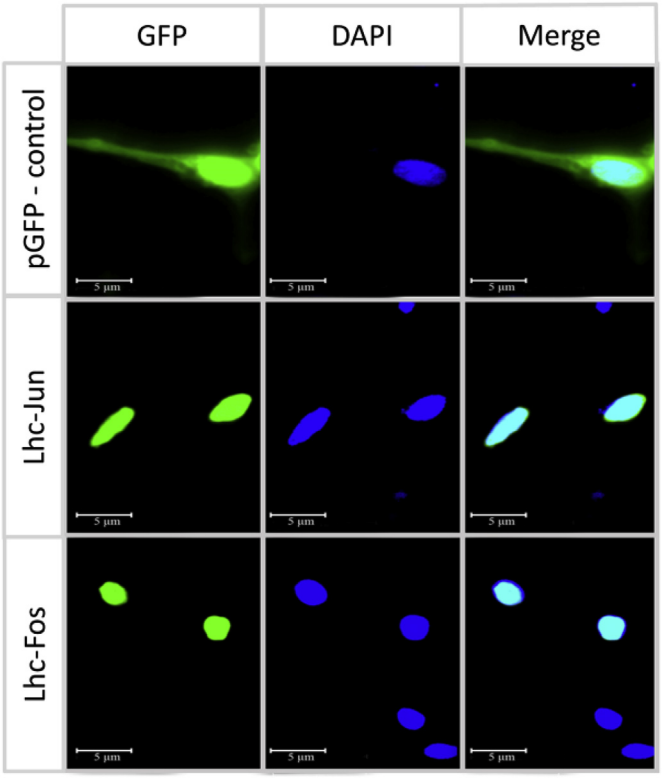


**Fig. 6.** Subcellular localization of Lhc-Jun and Lhc-Fos in mullet kidney cells after 24 h posttransfection incubation. Cells transfected with empty pEGFPN-1 was used as a control. DAPI staining showed the nuclei of cells. Images were taken using fluorescence microscopy (Leica, Germany) with × 400 magnification.

Also, previous reports suggest that JNK1 is required for gene expression in macrophages through TLR1 and TLR2 heterodimer where JNK is involved in phosphorylation of c-Jun, which increases the AP-1 transcriptional activity [78]. The above reports and upregulation of *Lhc-Jun* and *Lhc-Fos* upon the *L. garvieae* challenge suggest that both genes are involved in the immune response against Gram-positive bacteria. Further extensive studies on AP-1 mediated leukocyte activation and the differentiation of the immune system suggest the role of AP-1 in acquired immunity [62]. All the results of this study and previous evidence indicate a potential strong part played by *Lhc-Jun* and *Lhc-Fos* in bacterial and viral pathogenic infection, triggering a wide array of immune responses in red lip mullet.

In order to elicit immune responses, cells must express immune responsive genes. For this expression, transcription factors or kinases which phosphorylate the transcription factors must be localized in the nucleus of the cell upon a transcriptional inducing signal by a signal transduction pathway [79]. The predicted nuclear localization signal (NLS) from both Lhc-Jun and Lhc-Fos indicates that both transcription factors are localized into the nucleus. An earlier study on teleost c-Jun has provided evidence for its nuclear localization in *Epinephelus coioides* [20]. Also, both c-Jun and c-Fos in *Litopenaeus vannamei* and Fos from *Crassostrea hongkongensis* have shown nuclear subcellular localization in expressed cells [22,25]. These reports as well as results of the subcellular localization assay performed in this study, confirmed the nuclear localization of both Lhc-Jun and Lhc-Fos, thus fulfilling one of the main requirements for the functionality of a transcription factor.

The excess amount of UV radiation, which results due to ozone depletion plays a critical effect in living organisms and entire ecosystems. There are several reports which emphasize the effect of UV radiation on aquatic life. The fish behavior, food chains, and immunity are mainly affected as a result of exposure to excess UV radiation [80–82]. Although there is a scarce in the molecular level studies on fish UV response, it is a well-established fact that AP-1 is involved in UV response in mammalian cells [83]. Previous studies have reported that both *c-Jun* and *c-Fos* genes are induced in mammalian cells on UV exposure [84,85]. For the first time, the teleost *c-Jun, c-Fos* gene

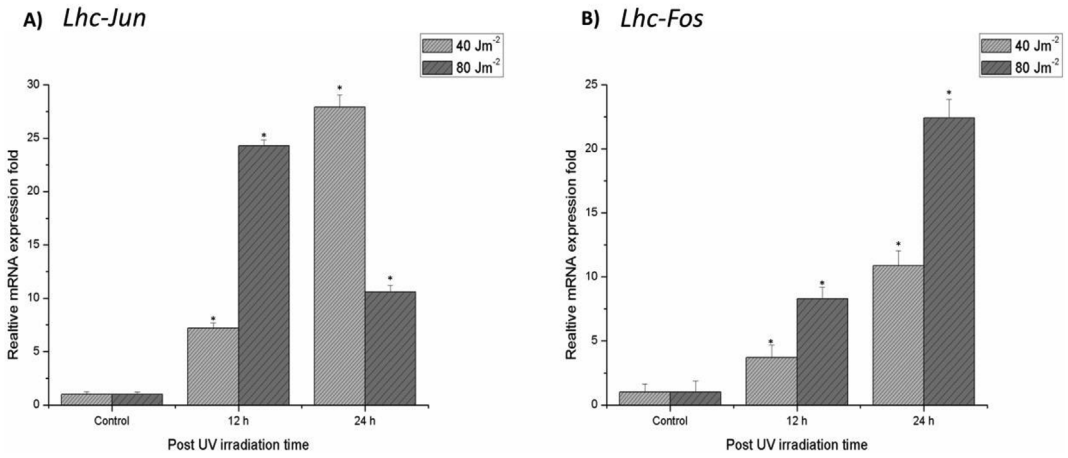


**Fig. 7.** The expression profiles of (A) *Lhc-Jun* and (B) *Lhc-Fos* genes upon UV irradiation. The mRNA expression was measured by qRT-PCR and evaluated by the Livak method. *Liza haematocheila* EF1-α was used as the internal control. Error bars represent standard deviation with experimental replicates (n = 3). Significant differences between challenged groups and 0 h control groups are indicated by an asterisk (*) ($P < 0.05$).

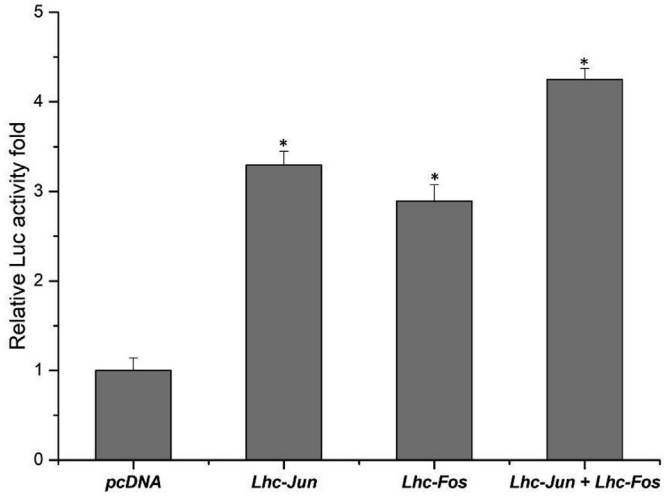


**Fig. 8.** The effect of Lhc-Jun and Lhc-Fos on AP-1 reporter activity in MK cells. MK cells were transiently co-transfected with AP-1-Luc reporter plasmid with *Lhc-Jun*-pcDNA™3.1(+) and *Lhc-Fos*-pcDNA™3.1(+) plasmids together with Renila luciferase (pRL-TK) plasmid as an internal control. Empty pcDNA™3.1(+) was used as a control. Significant differences are indicated by an asterisk (*) ($P < 0.05$).

expression after short wavelength UV exposure (UVC = 254 nm) has been examined in this report. The results suggest that *Lhc-Jun* and *Lhc-Fos* are stimulated in accordance with the energy dose and time. Both genes were observed to be upregulated after UV exposure. UVC is an active DNA damaging agent; this results in cell cycle arrest to repair the DNA or eliminate the cells which cannot be repaired [86,87]. Previous reports have claimed that c-Jun is involved in cell-cycle re-entry by negative regulation of the p53-mediated p21 expression [83]. Moreover, it has been reported that c-Fos is involved in re-expression of DNA repair genes including *xpf*, in a UV irradiated DNA lesion, and in re-installing the normal DNA repair mechanism in mouse embryonic fibroblasts [88]. In this study, *Lhc-Jun* showed a significant upregulation in the low energy (40 J $m^{-2}$) dose group with time, but in high energy (80 J $m^{-2}$) dosage, though it showed a significant upregulation, the increment of the expression at 24 h was comparatively lesser than the 12 h expression fold at low energy dose. This result may be due to the severe damage to the DNA by high dosage of UV. Cells may need more time to recover from the damage. As a result, cell-cycle re-entry was reduced by inducing cell cycle arrest. In the case of *Lhc-Fos*, the expression kept increasing with time and dosage increases suggesting the restoration of the DNA repairing mechanism. It showed the highest expression in the high dosage group at the 24 h time point, suggesting positive evidence for our first hypothesis about the *Lhc-Jun* decrement at the 24 h time point in the high dosage group. For the first time, these results demonstrated teleost *c-Jun* and *c-Fos* involvement in UV response suggesting the functional conservation of the proteins. Further studies are needed to confirm the above hypothesis.

The functionality of Lhc-Jun and Lhc-Fos were examined using the AP-1-Luc reporter assay. Results suggest that both Lhc-Jun and Lhc-Fos activated the AP-1 promoter in the AP-1-Luc reporter. The *Lhc-Jun* and *Lhc-Fos* co-transfected group showed the highest activity fold suggesting an enhancement of the AP-1 promoter activity. These results revealed that both Lhc-Jun and Lhc-Fos have the functionality to bind an AP-1 region of a gene and initiate transcription. Moreover, by suggesting the formation of the Lhc-Jun and Lhc-Fos (AP-1) dimer, which enhanced the activity of the AP-1 transcription factor, it was suggested that both Lhc-Jun and Lhc-Fos work together to augment AP-1. Previous studies on c-Jun and c-Fos have reported similar results in *Epinephelus coioides* [20], and *Crassostrea hongkongensis* [22,23]. All these results suggest that the AP-1 functionality is conserved in both Lhc-Jun and Lhc-Fos, indicating that *Lhc-Jun* and *Lhc-Fos* identified in *Liza haematocheila* are functionally active.

## 5. Conclusion

Lhc-Jun and Lhc-Fos posses a typical bZIP leucine zipper domain, which is involved in DNA binding and dimerization. The main phosphorylation sites and DNA binding sites of both genes have been conserved through evolution. *Lhc-Jun* and *Lhc-Fos* were ubiquitously expressed in all examined tissues and exhibited a robust response against immune stimulation. Both *Lhc-Jun* and *Lhc-Fos* showed a strong response to UV irradiation. This is the first study on UV irradiation response in *c-Jun*, *c-Fos* orthologs of fish. Both genes are nuclear-localized and induce AP-1 reporter gene expression, which is the main function of AP-1 transcription factors. All these data suggest that *Lhc-Jun* and *Lhc-Fos* are involved in MAPK signaling pathways and broaden our current knowledge of AP-1 structure and function.

## Acknowledgments

This research was part of the project titled “Fish Vaccine Research Center,” funded by the Ministry of Oceans and Fisheries, Korea and supported by a grant from Marine Biotechnology Program (20180430, Genome Analysis of Marine and Fisheries Organisms and Development of functional Application) Funded by Ministry of Oceans and Fisheries,

Korea.

## Appendix A. Supplementary data

Supplementary data related to this article can be found at https://doi.org/10.1016/j.fsi.2019.08.013.

## References


[1] P. Angel, M. Karin, The role of Jun, Fos and the AP-1 complex in cell-proliferation and transformation, BBA - Rev. Cancer. 1072 (1991) 129–157, https://doi.org/10.1016/0304-419X(91)90011-9.

[2] P.W. Vesely, P.B. Staber, G. Hoefler, L. Kenner, Translational regulation mechanisms of AP-1 proteins, Mutat. Res. Rev. Mutat. Res. 682 (2009) 7–12, https://doi.org/10.1016/j.mrrev.2009.01.001.

[3] M. Karin, E. Shaulian, AP-1: linking hydrogen peroxide and oxidative stress to the control of cell proliferation and death, IUBMB Life 52 (2001) 17–24, https://doi.org/10.1080/15216540252774711.

[4] R. Eferl, E.F. Wagner, AP-1: A double-edged sword in tumorigenesis, Nat. Rev. Cancer 3 (2003) 859–868, https://doi.org/10.1038/nrc1209.

[5] Y. Chinenov, T.K. Kerppola, Close encounters of many kinds: fos-Jun interactions that mediate transcription regulatory specificity, Oncogene 20 (2001) 2438–2452, https://doi.org/10.1038/sj.onc.1204385.

[6] M. Karin, The regulation of AP-1 activity by mitogen-activated protein kinases, Philos. Trans. R. Soc. Biol. Sci. 351 (1996) 127–134, https://doi.org/10.1098/rstb.1996.0008.

[7] L. Chang, M. Karin, Mammalian MAP kinase signalling cascades, Nature 410 (2001) 37–40, https://doi.org/10.1038/35065000.

[8] H.J. Zapata, M. Nakatsugawa, J.F. Moffat, Varicella-zoster virus infection of human fibroblast cells activates the c-Jun N-terminal kinase pathway, J. Virol. 81 (2007) 977–990, https://doi.org/10.1128/JVI.01470-06.

[9] R. Treisman, Regulation of transcription by MAP kinase cascades, Curr. Opin. Cell Biol. 8 (1996) 205–215, https://doi.org/10.1016/S0955-0674(96)80067-6.

[10] E. Shaulian, M. Karin, AP-1 as a regulator of cell life and death, Nat. Cell Biol. 4 (2002) E131–E136, https://doi.org/10.1038/ncb0502-e131.

[11] T. Curran, B.R. Franza, Fos and jun: the AP-1 connection, Cell 55 (1988) 395–397, https://doi.org/10.1016/0092-8674(88)90024-4.

[12] S. Fujioka, J. Niu, C. Schmidt, G.M. Sclabas, B. Peng, T. Uwagawa, Z. Li, D.B. Evans, J.L. Abbruzzese, P.J. Chiao, NF- B and AP-1 connection: mechanism of NF- B-dependent regulation of AP-1 activity, Mol. Cell. Biol. 24 (2004) 7806–7819, https://doi.org/10.1128/MCB.24.17.7806-7819.2004.

[13] R.P. Ryseck, R. Bravo, c-JUN, JUN B, and JUN D differ in their binding affinities to AP-1 and CRE consensus sequences: effect of FOS proteins, Oncogene 6 (1991) 533–542 http://www.ncbi.nlm.nih.gov/pubmed/1827665 , Accessed date: 6 September 2018.

[14] J. Kallio, A. Leinonen, J. Ulvila, S. Valanne, R.A. Ezekowitz, M. Rämet, Functional analysis of immune response genes in Drosophila identifies JNK pathway as a regulator of antimicrobial peptide gene expression in S2 cells, Microb. Infect. 7 (2005) 811–819, https://doi.org/10.1016/j.micinf.2005.03.014.

[15] S. Akira, Pathogen recognition by innate immunity and its signaling, Proc. Japan Acad. Ser. B Phys. Biol. Sci. 85 (2009) 143–156, https://doi.org/10.2183/pjab/85.143.

[16] O.N. Karpus, K.M. Heutinck, P.J.M. Wijnker, P.P. Tak, J. Hamann, Triggering of the dsRNA sensors TLR3, MDA5, and RIG-I induces CD55 expression in synovial fibroblasts, PLoS One 7 (2012) 3–10, https://doi.org/10.1371/journal.pone.0035606.

[17] I.M. Adcock, Transcription factors as activators of gene transcription: AP-1 and NF-kappa B, Monaldi Arch. Chest Dis. = Arch. Monaldi Mal. del Torace 52 (1997) 178–186 http://www.ncbi.nlm.nih.gov/pubmed/9203818 , Accessed date: 6 September 2018.

[18] Y. Nakabeppu, K. Ryder, D. Nathans, DNA binding activities of three murine Jun proteins: stimulation by Fos, Cell 55 (1988) 907–915 http://www.ncbi.nlm.nih.gov/pubmed/3142691 , Accessed date: 6 September 2018.

[19] G.L. Johnson, R. Lapadat, Mitogen-activated protein kinase pathways mediated by ERK, JNK, and p38 protein kinases, Science 298 (80) (2002) 1911–1912, https://doi.org/10.1126/science.1072682.

[20] S. Wei, Y. Huang, X. Huang, Q. Qin, Characterization of c-Jun from orange-spotted grouper, Epinephelus coioides involved in SGIV infection, Fish Shellfish Immunol. 43 (2015) 230–240, https://doi.org/10.1016/j.fsi.2014.12.033.

[21] M. De Zoysa, C. Nikapitiya, Y. Lee, S. Lee, C. Oh, I. Whang, S.Y. Yeo, C.Y. Choi, J. Lee, First molluscan transcription factor activator protein-1 (Ap-1) member from disk abalone and its expression profiling against immune challenge and tissue injury, Fish Shellfish Immunol. 29 (2010) 1028–1036, https://doi.org/10.1016/j.fsi.2010.08.014.

[22] F. Qu, Z. Xiang, F. Wang, Y. Zhang, Y. Tong, J. Li, Y. Zhang, Z. Yu, A novel molluscan Fos gene with immune defense function identified in the Hong Kong oyster, Crassostrea hongkongensis, Dev. Comp. Immunol. 51 (2015) 194–201, https://doi.org/10.1016/j.dci.2015.03.012.

[23] Z. Xiang, F. Qu, J. Li, L. Qi, Z. Yang, X. Kong, Z. Yu, Activator protein-1 (AP-1) and response to pathogen infection in the Hong Kong oyster (Crassostrea hongkongensis), Fish Shellfish Immunol. 36 (2014) 83–89, https://doi.org/10.1016/j.fsi.2013.10.005.

[24] D. Yao, L. Ruan, X. Xu, H. Shi, Identification of a c-Jun homolog from Litopenaeus vannamei as a downstream substrate of JNK in response to WSSV infection, Dev. Comp. Immunol. 49 (2015) 282–289, https://doi.org/10.1016/j.dci.2014.12.012.

[25] C. Li, H. Li, S. Wang, X. Song, Z. Zhang, Z. Qian, H. Zuo, X. Xu, S. Weng, J. He, The c-Fos and c-Jun from Litopenaeus vannamei play opposite roles in Vibrio parahaemolyticus and white spot syndrome virus infection, Dev. Comp. Immunol. 52 (2015) 26–36, https://doi.org/10.1016/j.dci.2015.04.009.

[26] G. Shi, C. Zhao, M. Fu, L. Qiu, The immune response of the C-Jun in the black tiger shrimp (Penaeus monodon) after bacterial infection, Fish Shellfish Immunol. 61 (2017) 181–186, https://doi.org/10.1016/j.fsi.2016.12.025.

[27] K.K. Perkins, A. Admon, N. Patel, R. Tjian, The Drosophila Fos-related AP-1 protein is a developmentally regulated transcription factor, Genes Dev. 4 (1990) 822–834, https://doi.org/10.1101/gad.4.5.822.

[28] S.K. Chanda, S. White, A.P. Orth, R. Reisdorph, L. Miraglia, R.S. Thomas, P. DeJesus, D.E. Mason, Q. Huang, R. Vega, D.-H. Yu, C.G. Nelson, B.M. Smith, R. Terry, A.S. Linford, Y. Yu, G. -w. Chirn, C. Song, M.A. Labow, D. Cohen, F.J. King, E.C. Peters, P.G. Schultz, P.K. Vogt, J.B. Hogenesch, J.S. Caldwell, Genome-scale functional profiling of the mammalian AP-1 signaling pathway, Proc. Natl. Acad. Sci. 100 (2003) 12153–12158, https://doi.org/10.1073/pnas.1934839100.

[29] J.R. Delaney, S. Stöven, H. Uvell, K. V Anderson, Y. Engström, M. Mlodzik, Cooperative control of Drosophila immune responses by the JNK and NF-κB signaling pathways, EMBO J. 25 (2006) 3068–3077, https://doi.org/10.1038/sj.emboj.7601182.

[30] C.A. Valenzuela, R. Zuloaga, M. Poblete-Morales, T. Vera-Tobar, L. Mercado, R. Avendaño-Herrera, J.A. Valdés, A. Molina, Fish skeletal muscle tissue is an important focus of immune reactions during pathogen infection, Dev. Comp. Immunol. 73 (2017) 1–9, https://doi.org/10.1016/j.dci.2017.03.004.

[31] E. Isern, M. Gustems, M. Messerle, E. Borst, P. Ghazal, A. Angulo, The activator protein 1 binding motifs within the human cytomegalovirus major immediate-early enhancer are functionally redundant and act in a cooperative manner with the NF-B sites during acute infection, J. Virol. 85 (2011) 1732–1746, https://doi.org/10.1128/JVI.01713-10.

[32] K. Machida, H. Tsukamoto, J.-C. Liu, Y.-P. Han, S. Govindarajan, M.M.C. Lai, S. Akira, J.-H.J. Ou, c-Jun mediates hepatitis C virus hepatocarcinogenesis through signal transducer and activator of transcription 3 and nitric oxide-dependent impairment of oxidative DNA repair, Hepatology 52 (2010) 480–492, https://doi.org/10.1002/hep.23697.

[33] C.-W. Chang, C.-S. Huang, W.-N. Tzeng, Redescription of redlip mullet Chelon haematocheilus (Pisces: Mugilidae) with a key to mugilid fishes in Taiwan, Acta Zool. Taiwanica 10 (1999) 0.

[34] A.V. Semina, N.E. Polyakova, M.A. Makhotkin, V.A. Brykov, Mitochondrial DNA divergence and phylogenetic relationships in mullets (pisces: Mugilidae) of the sea of Japan and the sea of azov revealed by PCR-RFLP-analysis, Russ. J. Mar. Biol. 33 (2007) 187–192, https://doi.org/10.1134/S1063074007030078.

[35] L. Hong, T. Fujita, T. Wada, H. Amano, N. Hiramatsu, X. Zhang, T. Todo, A. Hara, Choriogenin and vitellogenin in red lip mullet (Chelon haematocheilus):Purification, characterization, and evaluation as potential biomarkers for detecting estrogenic activity, Comp. Biochem. Physiol. C Toxicol. Pharmacol. 149 (2009) 9–17, https://doi.org/10.1016/j.cbpc.2008.05.017.

[36] S.F. Altschul, W. Gish, W. Miller, E.W. Myers, D.J. Lipman, Basic local alignment search tool, J. Mol. Biol. 215 (1990) 403–410, https://doi.org/10.1016/S0022-2836(05)80360-2.

[37] D.L. Wheeler, D.M. Church, S. Federhen, A.E. Lash, T.L. Madden, J.U. Pontius, G.D. Schuler, L.M. Schriml, E. Sequeira, T.A. Tatusova, L. Wagner, Database resources of the National Center for Biotechnology, Nucleic Acids Res. 31 (2003) 28–33, https://doi.org/10.1093/nar/gkg033.

[38] C.J.A. Sigrist, E. de Castro, L. Cerutti, B.A. Cuche, N. Hulo, A. Bridge, L. Bougueleret, I. Xenarios, New and continuing developments at PROSITE, Nucleic Acids Res. 41 (2012) D344–D347, https://doi.org/10.1093/nar/gks1067.

[39] A. Marchler-Bauer, Y. Bo, L. Han, J. He, C.J. Lanczycki, S. Lu, F. Chitsaz, M.K. Derbyshire, R.C. Geer, N.R. Gonzales, M. Gwadz, D.I. Hurwitz, F. Lu, G.H. Marchler, J.S. Song, N. Thanki, Z. Wang, R.A. Yamashita, D. Zhang, C. Zheng, L.Y. Geer, S.H. Bryant, CDD/SPARCLE: functional classification of proteins via subfamily domain architectures, Nucleic Acids Res. 45 (2017) D200–D203, https://doi.org/10.1093/nar/gkw1129.

[40] E. Gasteiger, C. Hoogland, A. Gattiker, S. Duvaud, M. Wilkins, R. Appel, A. Bairoch, Protein identification and analysis tools on the ExPASy server, Proteomics Protoc. Handb, 2005, pp. 571–607, , https://doi.org/10.1385/1-59259-890-0:571.

[41] K. Nakai, P. Horton, PSORT: a program for detecting sorting signals in proteins and predicting their subcellular localization, Trends Biochem. Sci. 24 (1999) 34–35, https://doi.org/10.1016/S0968-0004(98)01336-X.

[42] M.A. Larkin, G. Blackshields, N.P. Brown, R. Chenna, P.A. McGettigan, H. McWilliam, F. Valentin, I.M. Wallace, A. Wilm, R. Lopez, J.D. Thompson, T.J. Gibson, D.G. Higgins, Clustal W and clustal X version 2.0, Bioinformatics 23 (2007) 2947–2948, https://doi.org/10.1093/bioinformatics/btm404.

[43] P. Rice, I. Longden, A. Bleasby, EMBOSS: the European molecular biology open software suite, Trends Genet. 16 (2000) 276–277, https://doi.org/10.1016/S0168-9525(00)02024-2.

[44] S. Kumar, G. Stecher, K. Tamura, MEGA7: molecular evolutionary genetics analysis version 7.0 for bigger datasets, Mol. Biol. Evol. 33 (2016) 1870–1874, https://doi.org/10.1093/molbev/msw054.

[45] M. Källberg, H. Wang, S. Wang, J. Peng, Z. Wang, H. Lu, J. Xu, Template-based protein structure modeling using the RaptorX web server, Nat. Protoc. 7 (2012) 1511–1522, https://doi.org/10.1038/nprot.2012.085.

[46] A. Waterhouse, M. Bertoni, S. Bienert, G. Studer, G. Tauriello, R. Gumienny, F.T. Heer, T.A.P. de Beer, C. Rempfer, L. Bordoli, R. Lepore, T. Schwede, SWISS-MODEL: homology modelling of protein structures and complexes, Nucleic Acids

Res. 46 (2018) W296–W303, https://doi.org/10.1093/nar/gky427.
[47] W.L. DeLano, The PyMOL Molecular Graphics System, Version 1.8, Schrödinger LLC, 2002 citeulike-article-id:240061.
[48] S.A. Bustin, V. Benes, J.A. Garson, J. Hellemans, J. Huggett, M. Kubista, R. Mueller, T. Nolan, M.W. Pfaffl, G.L. Shipley, J. Vandesompele, C.T. Wittwer, The MIQE guidelines: Minimum information for publication of quantitative real-time PCR experiments, Clin. Chem. 55 (2009) 611–622, https://doi.org/10.1373/clinchem.2008.112797.
[49] K.J. Livak, T.D. Schmittgen, Analysis of relative gene expression data using real-time quantitative PCR and the $2-\Delta\Delta CT$ method, Methods (Duluth) 25 (2001) 402–408 10.1006.
[50] T. Kallunki, T. Deng, M. Hibi, M. Karin, c-Jun can recruit JNK to phosphorylate dimerization partners via specific docking interactions, Cell 87 (1996) 929–939, https://doi.org/10.1016/S0092-8674(00)81999-6.
[51] P. Monje, M.J. Marinissen, J.S. Gutkind, Phosphorylation of the carboxyl-terminal transactivation domain of c-fos by extracellular signal-regulated kinase mediates the transcriptional activation of AP-1 and cellular transformation induced by platelet-derived growth factor, Heal. (San Fr, 23 (2003) 7030–7043, https://doi.org/10.1128/MCB.23.19.7030.
[52] J.N.M. Glover, S.C. Harrison, Crystal structure of the heterodimeric bZIP transcription factor c-Fos–c-Jun bound to DNA, Nature 373 (1995) 257–261, https://doi.org/10.1038/373257a0.
[53] R. Wisdom, Ap-1: one switch for many signals, Exp. Cell Res. 253 (1999) 180–185, https://doi.org/10.1006/excr.1999.4685.
[54] C.R. Vinson, T. Hai, S.M. Boyd, Dimerization specificity of the leucine zipper-containing bZIP motif on DNA binding: prediction and rational design, Genes Dev. 7 (1993) 1047–1058, https://doi.org/10.1101/gad.7.6.1047.
[55] T.D. Halazonetis, K. Georgopoulos, M.E. Greenberg, P. Leder, c-Jun dimerizes with itself and with c-Fos, forming complexes of different DNA binding affinities, Cell 55 (1988) 917–924, https://doi.org/10.1016/0092-8674(88)90147-X.
[56] B.J. Pulverer, J.M. Kyriakis, J. Avruch, E. Nikolakaki, J.R. Woodgett, Phosphorylation of c-jun mediated by MAP kinases, Nature 353 (1991) 670–674, https://doi.org/10.1038/353670a0.
[57] M.N. Weitzmann, Bone and the immune system, Toxicol. Pathol. 45 (2017) 911–924, https://doi.org/10.1177/0192623317735316.
[58] I. Matsuoka, K. Fuyuki, T. Shoji, K. Kurihara, Identification of c-fos related genes and their induction by neural activation in rainbow trout brain, Biochim. Biophys. Acta Gene Struct. Expr. 1395 (1998) 220–227, https://doi.org/10.1016/S0167-4781(97)00164-4.
[59] Y. Li, J. Ma, Q. Fang, X. Li, *c-Fos* and *c-jun* expression in the liver of silver carp and the effect of microcystins, J. Biochem. Mol. Toxicol. 28 (2014) 157–166, https://doi.org/10.1002/jbt.21548.
[60] G. Thinakaran, J. Ojala, J. Bag, Expression of c- *jun*/AP-1 during myogenic differentiation in mouse $C_2C_{12}$ myoblasts, FEBS Lett. 319 (1993) 271–276, https://doi.org/10.1016/0014-5793(93)80561-8.
[61] J.I. Leu, M.A.S. Crissey, J.P. Leu, G. Ciliberto, R. Taub, Interleukin-6-Induced STAT3 and AP-1 amplify hepatocyte nuclear factor 1-mediated transactivation of hepatic genes, an adaptive response to liver injury, Mol. Cell. Biol. 21 (2001) 414–424, https://doi.org/10.1128/MCB.21.2.414-424.2001.
[62] V.C. Foletta, D.H. Segal, D.R. Cohen, Transcriptional regulation in the immune system: all roads lead to AP-1, J. Leukoc. Biol. 63 (1998) 139–152, https://doi.org/10.1002/jlb.63.2.139.
[63] J.Y. Kang, J.-O. Lee, Structural biology of the toll-like receptor family, Annu. Rev. Biochem. 80 (2011) 917–941, https://doi.org/10.1146/annurev-biochem-052909-141507.
[64] H.J. Han, N.S. Lee, M.S. Kim, S.H. Jung, An outbreak of lactococcus garvieae infection in cage-cultured red lip mullet chelon haematocheilus with green liver syndrome, Fish. Aquat. Sci. 18 (2015) 333–339, https://doi.org/10.5657/FAS.2015.0333.
[65] O. Byadgi, Y.-C. Chen, A.C. Barnes, M.-A. Tsai, P.-C. Wang, S.-C. Chen, Transcriptome analysis of grey mullet (Mugil cephalus) after challenge with Lactococcus garvieae, Fish Shellfish Immunol. 58 (2016) 593–603, https://doi.org/10.1016/j.fsi.2016.10.006.
[66] G.J. Lieschke, N.S. Trede, Fish immunology, Curr. Biol. 19 (2009) 678–682, https://doi.org/10.1016/j.cub.2009.06.068.
[67] A.-M. Möller, T. Korytář, B. Köllner, H. Schmidt-Posthaus, H. Segner, The teleostean liver as an immunological organ: intrahepatic immune cells (IHICs) in healthy and benzo[a]pyrene challenged rainbow trout (Oncorhynchus mykiss), Dev. Comp. Immunol. 46 (2014) 518–529, https://doi.org/10.1016/j.dci.2014.03.020.
[68] W. Liu, X. Ouyang, J. Yang, J. Liu, Q. Li, Y. Gu, M. Fukata, T. Lin, J.C. He, M. Abreu, J.C. Unkeless, L. Meyer, H. Xiong, AP-1 activated by toll-like receptors regulates expression of IL-23 p19, J. Biol. Chem. 284 (2009) 24006–24016, https://doi.org/10.1074/jbc.M109.025528.
[69] M.J. Smolinska, T.H. Page, A.M. Urbaniak, B.E. Mutch, N.J. Horwood, Hck tyrosine kinase regulates TLR4-induced TNF and IL-6 production via AP-1, J. Immunol. 187 (2011) 6043–6051, https://doi.org/10.4049/jimmunol.1100967.
[70] J. Kim, S. Woolridge, R. Biffi, E. Borghi, Members of the AP-1 family, c-Jun and c-Fos, functionally interact with JC virus early regulatory protein large T antigen, J. Virol. 77 (2003) 5241–5252, https://doi.org/10.1128/JVI.77.9.5241.
[71] Z. Zhou, B. Zhang, L. Sun, Poly(I:C) induces antiviral immune responses in Japanese flounder (Paralichthys olivaceus) that require TLR3 and MDA5 and is negatively regulated by Myd88, PLoS One 9 (2014) e112918, , https://doi.org/10.1371/journal.pone.0112918.
[72] K.-G. Lee, S. Xu, Z.-H. Kang, J. Huo, M. Huang, D. Liu, O. Takeuchi, S. Akira, K.-P. Lam, Bruton's tyrosine kinase phosphorylates Toll-like receptor 3 to initiate antiviral response, Proc. Natl. Acad. Sci. 109 (2012) 5791–5796, https://doi.org/10.1073/pnas.1119238109.
[73] C. Dong, D.D. Yang, M. Wysk, A.J. Whitmarsh, R.J. Davis, R.A. Flavell, Defective T cell differentiation in the absence of Jnk1, Science 282 (1998), https://doi.org/10.1126/SCIENCE.282.5396.2092 2092–5.
[74] T. Nakanishi, Y. Shibasaki, Y. Matsuura, T cells in fish, Biology (Basel) 4 (2015) 640–663, https://doi.org/10.3390/biology4040640.
[75] S.C. Chen, L.L. Liaw, H.Y. Su, S.C. Ko, C.Y. Wu, H.C. Chaung, Y.H. Tsai, K.L. Yang, Y.C. Chen, T.H. Chen, G.R. Lin, S.Y. Cheng, Y.D. Lin, J.L. Lee, C.C. Lai, Y.J. Weng, S.Y. Chu, Lactococcus garvieae, a cause of disease in grey mullet, Mugil cephalus L., in Taiwan, J. Fish Dis. 25 (2002) 727–732, https://doi.org/10.1046/j.1365-2761.2002.00415.x.
[76] M. Türe, H.İ. Haliloğlu, C. Altuntaş, H. Boran, İ. Kutlu, Comparison of experimental susceptibility of rainbow trout (Oncorhynchus mykiss), turbot (Psetta maxima), black sea trout (Salmo trutta labrax) and sea bass (Dicentrarchus labrax) to Lactococcus garvieae, Turk. J. Fish. Aquat. Sci. 14 (2014) 507–513, https://doi.org/10.4194/1303-2712-v14_2_22.
[77] O. Takeuchi, K. Hoshino, T. Kawai, H. Sanjo, H. Takada, T. Ogawa, K. Takeda, S. Akira, Differential roles of TLR2 and TLR4 in recognition of gram-negative and gram-positive bacterial cell wall components, Immunity 11 (1999) 443–451, https://doi.org/10.1016/S1074-7613(00)80119-3.
[78] H. Izadi, A.T. Motameni, T.C. Bates, E.R. Olivera, V. Villar-Suarez, I. Joshi, R. Garg, B.A. Osborne, R.J. Davis, M. Rincón, J. Anguita, c-Jun N-terminal kinase 1 is required for Toll-like receptor 1 gene expression in macrophages, Infect. Immun. 75 (2007) 5027–5034, https://doi.org/10.1128/IAI.00492-07.
[79] M.S. Cyert, Regulation of nuclear localization during signaling, J. Biol. Chem. 276 (2001), https://doi.org/10.1074/jbc.R100012200 20805–8.
[80] A.K. Manek, M.C.O. Ferrari, J.M. Sereda, S. Niyogi, D.P. Chivers, The effects of ultraviolet radiation on a freshwater prey fish: physiological stress response, club cell investment, and alarm cue production, Biol. J. Linn. Soc. 105 (2012) 832–841, https://doi.org/10.1111/j.1095-8312.2011.01829.x.
[81] D.P. Häder, C.E. Williamson, S.Å. Wängberg, M. Rautio, K.C. Rose, K. Gao, E.W. Helbling, R.P. Sinha, R. Worrest, Effects of UV radiation on aquatic ecosystems and interactions with other environmental factors, Photochem. Photobiol. Sci. 14 (2015) 108–126, https://doi.org/10.1039/c4pp90035a.
[82] H.M. Salo, E.I. Jokinen, S.E. Markkula, T.M. Aaltonen, H.T. Penttilä, Comparative effects of UVA and UVB irradiation on the immune system of fish, J. Photochem. Photobiol. B Biol. 56 (2000) 154–162, https://doi.org/10.1016/S1011-1344(00)00072-5.
[83] E. Shaulian, M. Schreiber, F. Piu, M. Beeche, E.F. Wagner, M. Karin, The mammalian UV response: c-Jun induction is required for exit from p53-imposed growth arrest, Cell 103 (2000) 897–907, https://doi.org/10.1016/S0092-8674(00)00193-8.
[84] R.M. Tyrrell, Activation of mammalian gene expression by the UV component of sunlight–from models to reality, Bioessays 18 (1996) 139–148, https://doi.org/10.1002/bies.950180210.
[85] P.K. Roddey, M. Garmyn, H.Y. Park, J. Bhawan, B.A. Gilchrest, Ultraviolet irradiation induces c-fos but not c-ha-ras proto-oncogene expression in human epidermis, J. Investig. Dermatol. 102 (1994) 296–299, https://doi.org/10.1111/1523-1747.ep12371785.
[86] W.K. Kaufmann, S.J. Wilson, G1 arrest and cell-cycle-dependent clastogenesis in UV-irradiated human fibroblasts, Mutat. Res. 314 (1994) 67–76 http://www.ncbi.nlm.nih.gov/pubmed/7504193 , Accessed date: 11 October 2018.
[87] X. Lu, D.P. Lane, Differential induction of transcriptionally active p53 following UV or ionizing radiation: defects in chromosome instability syndromes? Cell 75 (1993) 765–778 http://www.ncbi.nlm.nih.gov/pubmed/8242748 , Accessed date: 11 October 2018.
[88] M. Christmann, M.T. Tomicic, J. Origer, D. Aasland, B. Kaina, c-Fos is required for excision repair of UV-light induced DNA lesions by triggering the re-synthesis of XPF, Nucleic Acids Res. 34 (2006) 6530–6539, https://doi.org/10.1093/nar/gkl895.